Universal density scaling of disorder-limited low-temperature conductivity in high-mobility two-dimensional systems

S. Das Sarma[1] and E. H. Hwang[1,2]

[1] *Condensed Matter Theory Center, Department of Physics, University of Maryland, College Park, Maryland 20742-4111*
[2] *SKKU Advanced Institute of Nanotechnology and Department of Physics, Sungkyunkwan University, Suwon 440-746, Korea*

(Dated: April 18, 2013)

We theoretically consider the carrier density dependence of low-temperature electrical conductivity in high-quality and low-disorder two-dimensional (2D) "metallic" electronic systems such as 2D GaAs electron or hole quantum wells or doped/gated graphene. Taking into account resistive scattering by Coulomb disorder arising from quenched random charged impurities in the environment, we show that the 2D conductivity $\sigma(n)$ varies as $\sigma \sim n^{\beta(n)}$ as a function of the 2D carrier density n where the exponent $\beta(n)$ is a smooth, but non-monotonic, function of density n with possible nontrivial extrema. In particular, the density scaling exponent $\beta(n)$ depends qualitatively on whether the Coulomb disorder arises primarily from remote or background charged impurities or short-range disorder, and can, in principle, be used to characterize the nature of the dominant background disorder. A specific important prediction of the theory is that for resistive scattering by remote charged impurities, the exponent β can reach a value as large as 2.7 for $k_F d \sim 1$, where $k_F \sim \sqrt{n}$ is the 2D Fermi wave vector and d is the separation of the remote impurities from the 2D layer. Such an exponent β ($> 5/2$) is surprising because unscreened Coulomb scattering by remote impurities gives a limiting theoretical scaling exponent of $\beta = 5/2$, and näively one would expect $\beta(n) \leq 5/2$ for all densities since unscreened Coulomb scattering should nominally be the situation bounding the resistive scattering from above. We find numerically and show theoretically that the maximum value of α (β), the mobility (conductivity) exponent, for 2D semiconductor quantum wells is around 1.7 (2.7) for all values of d (and for both electrons and holes) with the maximum α occurring around $k_F d \sim 1$. We discuss experimental scenarios for the verification of our theory.

I. INTRODUCTION

It is well-known that carrier scattering by background quenched disorder arising from random impurities and defects limits the $T = 0$ (i.e., low-temperature) residual conductivity of a metal or doped semiconductor. This "residual resistivity", i.e., the extrapolated $T = 0$ value of the electrical resistivity obtained from the measured low-temperature transport data, provides information about the extrinsic disorder in the material limiting transport properties. In 3D metals, this residual resistivity is not of much intrinsic fundamental interest except for the fact that very pure defect-free single crystals, where the background disorder is presumably very low, could have extremely low residual resistivity leading to very long electron mean free paths. In particular, the residual resistivity of different samples (with different levels of sample purity, i.e., different impurity or defect content) of the same metal could differ by orders of magnitude, and a metallic resistivity uniquely defining a particular metal (e.g. Cu, Al, or Ag) is only meaningful at higher temperatures ($\gtrsim 100$ K) where phonon scattering dominates the electrical resistivity over impurity/defect/disorder scattering. At low temperatures, each metallic sample would have a unique resistivity reflecting its specific impurity content signature, and as such characterizing a metal by a unique resistivity is useless at low temperatures (i.e., each sample of the same metal would have different resistivity at $T = 0$). In fact, the low-temperature resistivity of a particular sample typically depends on the preparation history of the sample, and annealing to room temperatures (where all samples of a particular metal do have the same resistivity) and then cooling down to low temperatures could substantially modify the sample resistivity as the impurity/disorder configuration could change due to annealing. Theoretical statements[1] about residual resistivity (or equivalently, low temperature resistivity) of 3D metals thus focus on first principles calculations of the quantitative aspects of the local disorder potential arising from various defects or disorder in the metal (where the specific types of defect or impurity have to be specifically assumed), and then estimating the resistivity arising from various postulated disorder in terms of resistivity due to some specified impurity or defect content on an atomic percentage basis. Typical values of calculated residual resistivity for most simple metals fall in the $\sim 0.1 - 1$ $\mu\Omega$cm range per atomic percentage of impurities, and thus a metal with 99.999% (e.g., Cu) purity could have an extremely low residual resistivity of 10^{-10} Ωcm, leading to elastic mean free paths ~ 1 cm although the typical phonon-limited room-temperature mean free paths in most metals are only $1 - 10$ Å with the room-temperature phonon-limited resistivity of most metals being around $\sim \mu\Omega$cm.

Thus, theoretical studies[1,2] of disorder-limited residual resistivity of metals focus entirely on the quantitative modeling of various defect scattering in the metal using detailed materials-specific band structure and Boltz-

mann transport theories. No systematic dependence of the residual resistivity of metals on various metallicity parameters (e.g., the Wigner-Seitz radius r_s or lattice constant or Fermi energy) can in general be discussed qualitatively, and there is no metallic density scaling of conductivity that one can speak of since the carrier density cannot be tuned by an external gate voltage in metals (as it can be in 2D semiconductor systems or in graphene). In principle, there is only a modest variation in r_s ($\sim 2-6$) among different 3D metals (since $r_s \sim n^{-1/3}$ where n is the effective metallic free electron density), but the band structure variation in going from a metal to another would typically swamp any systematic r_s-dependence of the residual resistivity. Thus, the only systematic trend of the residual resistivity in metals which is discussed in the literature[1,2] is the dependence of the $T = 0$ impurity-limited resistivity of a particular metal on the atomic type (e.g. atomic number) of the various impurities or on the type of defects causing the resistive scattering. It is basically a subject of quantitative details based on serious numerical calculations.

In the current work we are interested in discussing qualitatively the impurity-limited 'metallic' residual (i.e. $T = 0$) resistivity as a function of the electron density of the metal. In particular, we want to understand the density-dependence of the $T = 0$ metallic resistivity assuming that the metallic density can be tuned continuously keeping all other parameters (e.g., disorder, band structure) fixed. Of course, such a situation is practically impossible in 3D metals since the electron density is fixed in each metal and cannot be tuned at all. But, as is well-known, such a tunable carrier density situation is routine in 2D "metallic" systems such as Si MOSFETs, gated semiconductor heterostructures and quantum wells, and gated graphene. In principle, a variable carrier density can be achieved in 3D doped semiconductor systems by changing the doping level (but keeping the same dopant element) in different samples, but this is not ideal for our purpose of a qualitative understanding of the density scaling of the metallic $T = 0$ saturated resistivity since there is always the possibility of unknown sample to sample variation beyond just the carrier density variation since doping level cannot be tuned continuously in a single sample as can be done in 2D systems. We do, however, briefly consider the density scaling properties of 3D impurity-limited saturated resistivity for the sake of completeness although most of the current work focuses on 2D semiconductor structures (and graphene) where the carrier density can be easily tuned in the same sample by applying an external gate voltage, and thus the density-dependent conductivity is a meaningful concept in 2D "effective metallic" systems existing in semiconductor structures and graphene.

Obviously, the $T = 0$ conductivity ($\equiv \rho^{-1}$, where ρ is resistivity) would manifest different density dependence for different types of background disorder, i.e., different types of impurity-electron interaction. The main resistive disorder scattering in relatively pure 3D metals is due to defects, vacancies, and impurities which scatter primarily through the short-range (essentially) δ-function type scattering potential (although there are extended defects which could produce anisotropic longer-range disorder potential). Disorder scattering by δ-function type point scatterers gives rise to rather uninteresting density scaling of electrical conductivity, again making 3D metals unsuitable for studying the density dependence of conductivity. Our main interest in this work is to obtain the density scaling of 2D $T = 0$ "metallic" conductivity arising from Coulomb disorder induced by random quenched charged impurity centers in the environment. Quenched Coulomb disorder is the dominant extrinsic resistive scattering mechanism in all semiconductor systems (2D or 3D) at low temperatures since doping by impurities is essential in inducing carriers in a semiconductor (whereas metals, by definition, have free carriers at the Fermi level even at $T = 0$), leading to the inevitable existence of background Coulomb disorder. Thus, a key distinction between low-temperature transport in metals and semiconductors is that short-range disorder (arising from very strong metallic screening) dominates metallic transport whereas long-range Coulombic disorder (arising from random localized charged impurities) dominates transport in (both 2D and 3D) doped semiconductors. The density dependent conductivity in doped semiconductor structures (or graphene) arises from the carrier screening of background Coulombic disorder which depends sensitively on the dimensionless ratio $q_{TF}/2k_F$ where q_{TF} and k_F are respectively the (density dependent) screening wave vector and Fermi wave vector of the system. The variation in the carrier screening properties as a function of the carrier density eventually leads to the density dependence of the resistivity.

Of course in doped semiconductors, one must worry about the additional complications of disorder-induced Anderson localization and/or low-temperature carrier freezeout and/or possible percolation transition associated with charged impurity-induced charge puddle formation. In the current work, we ignore all of these complications uncritically, focusing primarily on extremely high-quality modulation-doped 2D GaAs quantum well structures (and high-quality suspended graphene) where these complicating circumstances are absent down to very low carrier densities and very low temperatures. Our theoretical results presented in this paper, based on Drude-Boltzmann semiclassical transport theory, should apply to experimental systems above carrier densities (and temperatures) where localization (and related effects) become operational. The neglect of carrier localization and freezeout is not a particularly significant issue for our 2D theory and results because high-quality 2D semiconductor systems (and graphene) are not susceptible to these problems except perhaps at extremely low temperatures and carrier densities of little practical or experimental interest. On the other hand, our low-temperature and low-density transport results for 3D doped semiconductors are given here purely for the pur-

pose of completeness and comparison with 2D results since 3D doped semiconductors typically become insulating at low carrier density (as well as low temperature) because of localization and carrier freezeout. Our focus and most of our presented results, as the title of our article clearly indicates, are on low-temperature density dependent metallic transport properties of very high-quality 2D systems where the concept of density scaling of conductivity is both theoretically and experimentally meaningful.

One may wonder about the fact that the scaling theory of localization predicts that all 2D systems are strictly speaking Anderson insulators, and have, in principle, zero conductivity at $T = 0$ for infinite samples at all carrier densities. (This is theoretically true even for graphene when disorder induced intervalley carrier scattering is taken into account.) For our purpose in the current work, where we are specifically interested in very high-mobility 2D structures with very low background disorder, the scaling localization is a non-issue because (1) the samples are finite in size and the temperature, although low, is still finite; and (2) more importantly, the elastic mean free path is extremely long, making the effective 2D localization length much larger than the system size (or the phase breaking length, whichever is shorter). Thus, we are specifically considering the density dependence of the semiclassical part of the 2D resistivity in the situation where the semiclassical resistivity is much larger than the quantum (or weak localization) contribution to the resistivity. This limit is generic in high mobility 2D GaAs semiconductor systems and in graphene, and therefore our work is of wide validity. Thus we are strictly speaking considering the density dependence of the zeroth order semiclassical conductivity in the situation where the quantum contribution to the resistivity is negligible.

We emphasize that the density dependence (or scaling) of electrical transport properties is rarely discussed in the theoretical literature mainly because (as discussed above) such a density dependence of electrical conductivity is neither relevant nor interesting in 3D metals. Indeed, it is universally believed that the only aspect of electrical conductivity where studying the carrier density dependence is a meaningful endeavor is in the study of density-tuned Anderson localization as a ($T = 0$) quantum phase transition, exactly the physical phenomenon we are excluding in the current work where we focus entirely on the Drude-Boltzmann part of the conductivity in high quality samples assuming quantum localization effects to be negligible. Thus, the density scaling of our theory is not connected with quantum criticality at all, but with the behavior of the density dependence of the background disorder arising from nontrivial screening properties. In contrast to the density dependence which is rarely discussed in the literature except in the context of metal-insulator transition, the temperature dependence of transport properties has been extensively discussed for electronic materials (including many experimental and theoretical papers in 2D systems[3–7]) because the temperature dependent electrical resistivity generically contains qualitative information about the underlying resistive scattering mechanism. For example, a linear-in-T higher temperature metallic resistivity is the hallmark of acoustic phonon scattering in both metals and semiconductors (and in both 2D or 3D systems) whereas acoustic phonons typically lead to strongly suppressed high power laws ($\sim T^\eta$ with $\eta \approx 4-7$ depending on the details) in the (2D or 3D) metallic resistivity below a system-dependent Bloch-Grüneisen temperature T_{BG}. Our current work focuses entirely on temperatures well below the Bloch-Grüneisen temperature ($T \ll T_{BG}$) so that phonons are completely ineffective in limiting the electrical conductivity. Optical phonons, which are often relevant in semiconductor transport at higher temperatures and indeed limit the room-temperature resistivity of 2D GaAs-based semiconductor structures[8] and are exponentially suppressed as $e^{-\hbar\omega_{LO}/k_BT}$ at low temperatures (where $\hbar\omega_{LO} \sim 450$ K in GaAs), are completely irrelevant for our low-temperature transport considerations.

It is well-known that high-quality low-density 2D semiconductor systems (as well as graphene) often manifest a strong temperature dependence in its low-temperature resistivity[3–7], which arises from the strong temperature dependence of the screened Coulomb disorder[9] at low carrier densities. Again, our theoretical work at $T = 0$ is completely free from any temperature-induced complications in the resistivity since our interest is in understanding the density dependence of the $T = 0$ resistivity/conductivity, which can be obtained from the low-temperature experimental data by extrapolation to $T = 0$ or by sitting always at a constant very low temperature (e.g., 50 mK) in obtaining the density dependence of the transport properties. In any case, the question we are interested in is perfectly well-defined as a matter of principle: How does the $T = 0$ Drude-Boltzmann semiclassical conductivity of a 2D (or 3D) "metallic" system vary as a function of its carrier density in the presence of background screened Coulomb disorder being the main resistive scattering mechanism?

In the rest of this article, we provide a detailed theoretical answer to the question posed in the last sentence above.

II. BACKGROUND

The $T = 0$ conductivity $\sigma(n)$ of a 2D metallic system is typically written as[9,10]

$$\sigma(n) = \frac{e^2 v_F^2}{2} D(E_F)\tau(E_F), \tag{1}$$

in the Boltzmann theory, where E_F, v_F are respectively the Fermi energy and the Fermi velocity, $D(E_F)$ is the carrier density of states at the Fermi surface, and τ is the so-called relaxation time (or the scattering time) for

the relevant resistive scattering mechanism. (The factor 2 in the denominator of Eq. (1) is replaced by 3 for 3D systems.) It is assumed that v_F, E_F, and D are known as a function of the carrier density n from the relevant band structure information (and we will consider only the parabolic and the linear band approximation with the linear approximation used for obtaining our graphene transport results). The whole theory then boils down to a calculation of the transport relaxation time τ at the Fermi surface using the appropriate microscopic scattering mechanism (which we describe in details in section III of our paper).

For parabolic bands with $E(\mathbf{k}) = \hbar^2 k^2/2m$ we can write $E_F = mv_F^2/2$, where m is the carrier effective mass, and Eq. (1) simply reduces to the celebrated Drude-Boltzmann transport formula:

$$\sigma(n) = \frac{ne^2\tau}{m}, \tag{2}$$

where $\tau \equiv \tau(E_F)$ and n is the relevant (2D or 3D) carrier density. For graphene, Eq. (2) requires a slight modification[9] which we will discuss later when we come to describing our graphene results. From this point on, unless otherwise stated, our explicit equations and formula are given for parabolic band 2D systems — we will consider the very special linear band case of graphene separately at the appropriate juncture. Most of our results focus on 2D semiconductor systems, specifically 2D GaAs electron or hole quantum wells where the parabolic approximation applies well. We will point out the corresponding 3D parabolic band analytic results as appropriate, concentrating on presenting the equations and formulas mainly for 2D quantum well systems since most of our presented results are for 2D semiconductor systems, where the corresponding experiments are feasible.

We note that one can, instead of discussing the conductivity σ, equivalently discuss the relaxation time τ or the resistivity $\rho = \sigma^{-1}$ or the mobility μ, which is defined as

$$\mu = \frac{e\tau}{m} = \frac{\sigma}{ne}. \tag{3}$$

Obtaining the density dependent conductivity $\sigma(n)$ now becomes equivalent to obtaining the density dependence of τ or μ since $\sigma \propto n\mu$ (or $n\tau$). We write:

$$\tau \propto n^{\alpha}, \;\; \text{i.e.,} \;\; \mu \propto n^{\alpha}, \tag{4}$$

and therefore

$$\sigma \sim n^{\beta=\alpha+1}. \tag{5}$$

In general, we can define the conductivity exponent β, or equivalently the mobility exponent α through the relation:

$$\alpha(n) = \frac{d\ln\mu}{d\ln n}, \tag{6}$$

and

$$\beta(n) = \alpha(n) + 1 = \frac{d\ln\sigma}{d\ln n}. \tag{7}$$

We note that, in general, the mobility exponent $\alpha \equiv \alpha_\mu$ and the relaxation rate exponent α_τ may be unequal (e.g., graphene) except that for parabolic bands we have $\alpha_\mu = \alpha_\tau = \alpha$. But the relation $\beta = \alpha_\mu + 1 = \alpha + 1$ always applies. The main goal of the current work is to calculate the exponent $\alpha(n)$ for various specified disorder mechanism, and discuss/contrast how the density scaling exponent depends on the type of disorder controlling the resistive scattering mechanism.

We will obtain $\alpha(n)$ analytically in various limiting situations in our theoretical study. But the main technique would be to obtain $\mu(n)$ or $\sigma(n)$ numerically from the Boltzmann theory and then to calculate $\alpha(n)$ or $\beta(n)$. Experimentally, the way to estimate the exponent $\alpha(n)$ is to plot the measured low-temperature $\mu(n)$ against n, and then to estimate $\alpha(n)$ by carrying out the logarithmic differentiation. In general, $\alpha(n)$ will depend strongly on the background disorder, and will vary smoothly as a function of carrier density as different scattering mechanisms are operational in different density regimes and as the background Coulomb disorder is screened differently at different carrier density through the variation in $q_{TF}/2k_F$. An important surprising finding of our theory is an interesting nonmonotonic variation in the scaling exponent $\alpha(n)$ as a function of carrier density.

It is important to point out at this stage that graphene, because of its linear dispersion with a constant Fermi velocity ($v_F \equiv v_0$), does not obey[9] the exponent scaling relation $\beta = \alpha_\tau + 1$ connecting the density scaling between conductivity (β) and relaxation rate (α_τ). Instead, for graphene[9], we have $\beta = \alpha_\tau + 1/2$ if α_τ is defined by $\tau^{-1} \sim n^{\alpha_\tau}$ which follows from the constancy of v_F and the fact that $D(E_F) \propto E_F \propto \sqrt{n}$ in graphene. Putting $D(E_F) \propto k_F \propto \sqrt{n}$ in Eq. (17), we get for graphene $\sigma(n) \sim \sqrt{n}\tau(n)$, i.e., $\beta = \alpha_\tau + 1/2$. Thus, whereas in ordinary parabolic systems the exponent α ($\equiv \alpha_\tau \equiv \alpha_\mu$) is the same for both mobility (μ) and the relaxation rate (τ^{-1}), in graphene, by virtue of its linear band dispersion, $\alpha = \alpha_\mu = \alpha_\tau - 1/2$, but the relationship between the conductivity exponent (β) and the mobility exponent (α) is still given by $\beta = \alpha + 1$ since by definition $\sigma = ne\mu$.

III. MODEL AND THEORY

The central quantity to obtain theoretically in the semiclassical Boltzmann transport theory in the relaxation time τ or equivalently the relaxation rate τ^{-1}, which is given by the following expression for 2D systems, within the leading order Born approximation, for

carrier scattering at $T = 0$ by disorder[9,10]:

$$\frac{1}{\tau} = \frac{2\pi}{\hbar}\sum_{\gamma} \int N_i^{(\gamma)}(z)dz \int \frac{d^2k'}{(2\pi)^2}\left|V^{(\gamma)}_{\mathbf{k}-\mathbf{k}'}(z)\right|^2 \times (1-\cos\theta_{\mathbf{k}\mathbf{k}'})\delta[E(\mathbf{k})-E(\mathbf{k}')]. \quad (8)$$

Here $N_i^{(\gamma)}(z)$ is the 3D density of random impurities of the γ-th type (in general, there could be several different types of impurities present in the system: near and far, 2D or 3D, long- or short-range) with z being the direction perpendicular to the plane of 2D system (which lies in the x-y plane); $V_{\mathbf{q}}(z)$ is the electron-impurity interaction (in the 2D wave vector space defined by $\mathbf{q}$). $\mathbf{k}, \mathbf{k}'$ are the incoming and outgoing 2D carrier wave vectors involved in the scattering process with a scattering angle $\theta_{\mathbf{k}\mathbf{k}'}$ between them and $\mathbf{k}-\mathbf{k}'$ being the scattering wave vector; $E(\mathbf{k}) = \hbar^2k^2/2m$ is the carrier energy. Note that our disorder model assumes a random distribution of impurities in the 2D x-y plane although it is easy to include correlations in the 2D impurity distribution if experiment indicates the importance of such correlations.

Once the scattering potential $V_{\mathbf{q}}(z)$ is defined, the problem of calculating the 2D conductivity becomes simply a question of evaluating the 4-dimensional integral given in Eq. (8). Note that we are restricting to the $T = 0$ case (or to low temperatures), otherwise a thermal average would be required in defining τ^{-1} necessitating a 5-dimensional integration. We note that although Eq. (8) applies only to 2D systems, a very slight modification gives us the corresponding expressions for 3D systems and graphene, which we do not show here. We note here that for graphene there is a well-known additional form factor of $(1+\cos\theta_{\mathbf{k}\mathbf{k}'})$ inside the integral in Eq. (8) arising from chirality[9].

It is worthwhile to point out here that the theoretical idea of a meaningful universal density scaling behavior of conductivity applies as a matter of principle only when the resistive scattering is dominated by a particular disorder mechanism. If there are many different types of disorder (i.e., several γ-types) contributing equivalently to the resistivity, then the net resistivity will be given by the Matthiessen's rule: $\tau^{-1}(n) = \sum_\gamma \tau_\gamma^{-1}(n)$, and $\rho(n) = \sum_\gamma \rho_\gamma(n)$, i.e., $\sigma^{-1}(n) = \sum_\gamma \sigma_\gamma^{-1}(n)$, where ρ_γ, σ_γ, τ_γ are respectively the resistivity, conductivity, scattering time for the γ-th type of disorder arising from $N_i^{(\gamma)}(z)$ in Eq. (8). In such a situation, unless one particular type of disorder (i.e., one specific γ) dominates scattering, the resulting density dependence of the total σ (or μ) will manifest complex crossover behavior arising from the combination of all different scattering processes contributing with different strength, and there will not be only universal density dependent scaling behavior of $\sigma(n)$ or $\mu(n)$. To exemplify this important point, we consider a strict 2D electron gas being scattered by three different types of disorder (i.e., $\gamma = 1, 2, 3$) given by remote random charged impurities at a distance d from the 2D system, background charged impurities at the 2D layer, and zero-range disorder in the layer, each with their respective conductivity exponent β_γ with $\gamma = 1, 2, 3$ respectively. We can formally write:

$$\sigma^{-1}(n) = \sigma_1^{-1} + \sigma_2^{-1} + \sigma_3^{-1} = A_1 n^{-\beta_1} + A_2 n^{-\beta_2} + A_3 n^{-\beta_3}, \quad (9)$$

where $A_\gamma \propto n_{i,\gamma}$ is the strength of each independent physical scattering process (i.e., $n_{i,1}$, $n_{i,2}$, $n_{i,3}$ denote respectively the remote and background charged impurity density and the short-range defect density). If we now define the net conductivity exponent $\beta(n)$ through the usual $\beta = d\ln\sigma/d\ln n$ definition using the total conductivity $\sigma(n)$, then obviously $\beta(n)$ will be a complex (and opaque) function not only of β_1, β_2, and β_3, but also of the disorder strength $n_{i,1}$, $n_{i,2}$, $n_{i,3}$. Thus, the extraction of a *universal* density exponent β (or α) makes sense only when one scattering mechanism dominates — generically, the conductivity/mobility exponent β/α $(= \beta - 1)$ is nonuniversal and depends in a complex manner both on the individual scattering mechanism and the relative strengths of different operational scattering mechanisms.

We consider below theoretically several different disorder potentials which may be operational in real 2D and 3D systems, obtaining asymptotic analytical expressions for the exponent α and β in the process as applicable.

A. Zero-range disorder

Zero-range disorder, $V_{\mathbf{q}} \equiv V_0$ (a constant), corresponds to pure δ-function real space scatterers distributed randomly spatially. Without any loss of generality, we can drop the z-dependence of the disorder (since the electron-impurity interaction is spatially localized), and assume the 2D electron system to be of zero thickness in the z-direction interacting with the random zero-range scatterers situated in the same plane. For 3D systems we of course assume the scatterers to be randomly distributed three dimensionally.

For the constant $V_{\mathbf{q}}$ model potential it is straightforward to do the momentum integration in Eq. (8) to obtain the following results for 2D and 3D semiconductor systems and graphene:

$$\tau \sim n^0 \quad \text{2D}, \quad (10a)$$
$$\tau \sim n^{-1/3} \quad \text{3D}, \quad (10b)$$
$$\tau \sim n^{-1/2} \quad \text{graphene}. \quad (10c)$$

We note that in graphene the mobility exponent ($\alpha \equiv \alpha_\mu$) differs from the relaxation rate exponent α_τ by $\alpha_\mu = \alpha_\tau - 1/2$. In obtaining the density dependence of the relaxation time above we use the standard expressions for k_F and E_F for parabolic 2D, 3D systems, and graphene:

$$k_F = (2\pi n)^{1/2}; \quad E_F = \hbar^2\pi n/m : \text{ 2D}, \quad (11a)$$
$$k_F = (3\pi^2 n)^{1/3}; \; E_F = \hbar^2(3\pi^2 m)^{2/3}/2m : \text{ 3D}, \quad (11b)$$
$$k_F = (\pi n)^{1/2}; \quad E_F = \hbar v_0(\pi n)^{1/2} : \text{ graphene}. \quad (11c)$$

We use n throughout to denote the relevant 2D or 3D carrier density of the "metal", and v_0 in Eq. (11c) is the constant graphene Fermi velocity defining its linear energy-momentum relationship, $E = \hbar v_0 k$ ($v_0 \approx 10^8$ cm/s). We assume a spin degeneracy of 2 throughout and an additional valley degeneracy of 2 for graphene in defining k_F and E_F.

For zero-range δ-function disorder which is equivalent to assuming an uncorrelated white-noise disorder (often also called in the literature, "short-range disorder", somewhat misleadingly), we therefore have (we define $\alpha = \alpha_\mu$ always as the mobility exponent)

$$\alpha = 0 \ \text{(2D)}; \quad -1/3 \ \text{(3D)}; \quad -1 \ \text{(graphene)}, \tag{12}$$

and

$$\beta = \alpha + 1 = 1 \ \text{(2D)}; \quad 2/3 \ \text{(3D)}; \quad 0 \ \text{(graphene)}. \tag{13}$$

These results for 2D parabolic system and graphene are known[9,10] and show that the conductivity grows linearly with carrier density in 2D systems and becomes a density independent constant in graphene when transport is limited or dominated by zero-range white-noise type δ-function background disorder. The zero-range transport result for the 3D systems (metals or doped semiconductors) does not appear to be as well-known (perhaps because the density dependence of conductivity is not of much experimental interest in 3D systems as discussed in the Introduction of this paper) and shows surprisingly a sub-linear $\sim n^{2/3}$ increase in $\sigma(n)$ in 3D systems for δ-correlated short-range white-noise disorder.

We now move on to the more interesting and experimentally more relevant Coulomb disorder, and discuss a number of disorder models pertaining to Coulomb disorder in the next two subsections.

B. Unscreened (long-range) Coulomb disorder

In most semiconductor systems (2D or 3D), the dominant background disorder arises from quenched random charged impurities in the environment. Thus, the bare electron-impurity interaction is invariably the long-range $1/r$ Coulomb interaction arising from the electric potential of the charged impurity. The charged impurity could be an intentional dopant impurity introduced to provide the doping necessary to create free carriers in the semiconductor or an unintentional charged impurity invariably present even in the cleanest semiconductor. In general, the Coulomb disorder from the random charged impurities should be screened by the free carriers themselves so that the effective (screened) Coulomb disorder is short-ranged (this is the infra-red regularization necessary for handling the long range nature of Coulomb interaction). We consider the screened Coulomb disorder in the next three sub-sections, focusing here on the unscreened bare Coulomb disorder for the sake of theoretical completeness.

The disorder potential $V_{\mathbf{q}}(z)$ is given by the following equation for the unscreened Coulomb interaction:

$$V_{\mathbf{q}}(z) = \frac{2\pi Z e^2}{\kappa q} e^{-q|z|}, \tag{14}$$

for 2D systems and graphene, and

$$V_{\mathbf{q}}(z) = \frac{4\pi Z e^2}{\kappa q^2}, \tag{15}$$

for 3D systems. Here $q = |\mathbf{q}|$ in Eqs. (14) and (15) is the appropriate 2D and 3D wave vector, Z is the atomic number of the charged impurity center with Ze being its charge (we consider $Z = 1$ throughout), and κ is the background static lattice dielectric constant. The coordinate z in Eq. (14) denotes the spatial separation of the charged impurity from the 2D confinement plane of the electron layer (taken to be located at $z = 0$ in the x-y plane). We note that Eqs. (14) and (15) are simply the Fourier transform of the $1/r$ three-dimensional Coulomb interaction (with $\mathbf{r} \equiv (x, y, z)$ a 3D space vector) in 2D and 3D systems.

For 3D systems, unscreened Coulomb disorder leads to the following expression for the scattering rate:

$$\tau^{-1} = \frac{2\pi N_i}{\hbar} \int \frac{d^3k'}{(2\pi)^3} \left[\frac{4\pi e^2}{\kappa |\mathbf{k} - \mathbf{k}'|^2}\right]^2 \times (1 - \cos\theta_{\mathbf{k}\mathbf{k}'}) \delta(E_k - E_{k'}), \tag{16}$$

where all wave vectors are now three dimensional and N_i is the 3D impurity density. The momentum integration in Eq. (16) is straightforward, and it is well-known[11,12] that the integral has a logarithmic divergence arising from the long-range nature of bare Coulomb interaction (i.e., an infra-red singularity). We get:

$$\tau^{-1} \sim (n \ln b)^{-1} \to \infty, \tag{17}$$

with $b = 4k_F^2/q_{TF}^2 \to 0$, where $k_F = (3\pi^2 n)^{1/3}$, and q_{TF}, which in principle is the 3D screening wave vector, goes to zero in the unscreened approximation, leading to a logarithmic divergence without the screening cutoff of the long-range Coulomb interaction. There are several ways of cutting off this long-range logarithmic Coulomb divergence (e.g., Conwell-Weiskoff approximation or Brooks-Herring-Dingle approximation) which has been much discussed in the transport literature on doped semiconductors[11,12]. Since our interest in mainly focused on 2D systems where the carrier density can be tuned continuously (in contrast to 3D systems), we do not further discuss the implications of Eq. (17) for 3D doped semiconductors.

For 2D systems, one must distinguish among (at least) three different kinds of Coulomb disorder: Random 2D charged impurities in the 2D plane of the carriers [i.e., $z = 0$ in Eq. (14)], random charged impurities in a 2D layer parallel to the 2D carriers with a separation d (i.e. $z = d$), and 3D random charged impurity centers in the background (where z varies over a region in space).

We refer to these three situations as 2D near impurities, remote impurities, and 3D impurities, respectively, throughout this paper.

We first consider the 2D near impurity case with $z = 0$ assuming unscreened impurity-electron Coulomb interaction in the 2D plane:

$$V_q(z=0) = \frac{2\pi e^2}{\kappa q}. \tag{18}$$

This then gives (with n_i now as the 2D impurity density):

$$\tau^{-1} = \frac{2\pi n_i}{\hbar} \int \frac{d^2k'}{(2\pi)^2} \left[\frac{2\pi e^2}{\kappa|\mathbf{k}-\mathbf{k}'|}\right]^2 \times (1-\cos\theta_{\mathbf{kk}'})\delta(E_k - E_{k'}). \tag{19}$$

The 2D integral in Eq. (19), in contrast to the corresponding (divergent) 3D integral defined by Eq. (16), is convergent:

$$\tau^{-1} \sim k_F^{-2} \sim n^{-1}. \tag{20}$$

Thus $\alpha = 1$ in 2D systems for the unscreened 2D impurity case (while the corresponding 3D case is logarithmically divergent). The exponent $\beta = \alpha + 1 = 2$ for the unscreened 2D Coulomb impurity in 2D "metallic" systems.

Next we consider the 2D system with 2D remote impurities ($z = d \neq 0$). The relaxation rate [Eq. (8)] is now given by

$$\tau^{-1} = \frac{2\pi n_i}{\hbar} \int \frac{d^2k'}{(2\pi)^2} \left[\frac{2\pi e^2 e^{-|\mathbf{k}-\mathbf{k}'|d}}{\kappa|\mathbf{k}-\mathbf{k}'|}\right]^2 \times (1-\cos\theta_{\mathbf{kk}'})\delta(E_k - E_{k'}). \tag{21}$$

The integral in Eq. (21) can be rewritten in a dimensionless form

$$\tau^{-1} \sim k_F^{-2} \int_0^1 dx \frac{e^{-2xd_0}}{\sqrt{1-x^2}}, \tag{22}$$

where $d_0 = 2k_F d$ is dimensionless. [We note that putting $d_0 = 0$ for $d = 0$ gives us the 2D near impurity results of Eq. (20).] The asymptotic carrier density dependence ($k_F \propto \sqrt{n}$) implied by Eq. (22) depends sensitively on whether $k_F d$ [$\equiv d_0$ in Eq. (22)] is small ($k_F d \ll 1$) or large ($k_F d \gg 1$). For $k_F d \ll 1$, we get from Eq. (22)

$$\tau^{-1} \sim k_F^{-2} \sim n^{-1} \tag{23}$$

and for $k_F d \gg 1$, we get from Eq. (22)

$$\tau^{-1} \sim k_F^{-3} \sim n^{-3/2}. \tag{24}$$

Thus, $\alpha = 1$ (3/2) for $k_F d \ll 1$ ($\gg 1$) and therefore $\beta = 2$ (5/2) for $k_F d \ll 1$ ($\gg 1$) for 2D carriers in the presence of remote Coulomb scatterers.

Finally, we consider the 2D carrier system with a 3D random distribution of charged impurity centers. The integral for the 2D relaxation rate (Eq. (8)) now becomes with $q_{TF} \to 0$

$$\tau^{-1} \sim k_F^{-3} \ln\left(\frac{q_{TF}}{2k_F}\right) \sim n^{-3/2} \ln\left(\frac{q_{TF}}{2k_F}\right), \tag{25}$$

which has the same logarithmic divergence for the unscreened Coulomb disorder as the corresponding 3D case considered above in Eq. (17), but with a different 2D density exponent ($\sim n^{-3/2}$) from the corresponding 3D density exponent ($\sim n^{-1/3}$) in Eq. (17). Thus, 2D carrier systems with unscreened 3D Coulomb disorder would have logarithmically divergent resistivity necessitating a length cut-off on the long range part of the bare Coulomb potential similar to the well-known situation for long-range bare Coulomb disorder in 3D systems (e.g. doped semiconductors).

It is important to emphasize our interesting theoretical finding that, although 3D unscreened Coulomb disorder leads to logarithmic long-range divergence in the resistivity of both 2D and 3D systems independent of the carrier density (i.e. τ^{-1} diverges logarithmically), the corresponding situation for 2D carrier systems with 2D Coulomb disorder has no divergence and does not require any cut-off dependent infra-red regularization. It turns out that 2D metals with unscreened Coulomb disorder arising from random 2D charged impurities is perfectly well-defined within the Boltzmann transport theory. Of course, the unscreened Coulomb disorder model is not realistic and the calculated conductivity may not agree with the experimental data, but theoretically it is perfectly well-defined with the density exponents α (β) being 1 (3/2) and 2 (5/2), respectively depending on whether $k_F d \ll 1$ or $\gg 1$ where d is the location of the impurities with respect to the 2D carrier layer.

One may wonder about the fundamental reason underlying the necessity for infra-red regularization for the 3D unscreened case and *not* for the 2D unscreened case. This arises from the 3D bare Coulomb potential ($\sim 1/q^2$) being much more singular in the long wavelength $q \to 0$ limit than the corresponding 2D Coulomb potential ($\sim 1/q$). It turns out that this difference between 2D and 3D is sufficient to make the 3D Coulomb disorder case infra-red divergent whereas the 2D case being non-divergent without infra-red regularization.

We do not discuss here the unscreened Coulomb disorder case for graphene since for graphene the density scaling of the conductivity is the same for both unscreened and screened Coulomb disorder (and we consider screened Coulomb disorder in the next subsection) by virtue of graphene screening wave vector q_{TF} ($\propto k_F$) being proportional to the Fermi wave vector leading to both screened and unscreened Coulomb disorder having the same carrier density dependence in the conductivity.

C. Screened Coulomb Disorder

This is the most realistic (as well as reasonably computationally tractable) model for calculating the resistivity due to Coulomb scattering within the Boltzmann transport theory. The basic idea is to use the appropriately screened Coulomb potential in Eq. (8) for calculating the relaxation rate. We use the conceptually simplest (static) random phase approximation (RPA) for carrier screening of the long-range electron-impurity Coulomb interaction. This means that the screening functions in 2D and 3D parabolic systems are the static dielectric functions first calculated by Stern[13] and Linhard[14], respectively. For graphene, we use the dielectric screening function first calculated in Ref. [15].

The relevant screened Coulomb disorder potential is given by:

$$V_q \equiv \frac{v_q}{\epsilon(q)}, \tag{26}$$

where v_q is the long-range Coulomb potential and $\epsilon(q)$ is the appropriate static RPA dielectric function. In general, the screened Coulomb potential can be rewritten as

$$V_q = \frac{2\pi e^2}{\kappa(q+q_{TF})}, \tag{27}$$

for 2D systems and graphene, and

$$V_q = \frac{4\pi e^2}{\kappa(q^2+q_{TF}^2)}, \tag{28}$$

for 3D systems. The screening wave vector q_{TF}, sometimes referred to as the Thomas-Fermi wave vector is given by the following expression (obtained in a straightforward manner from the corresponding static polarizability function or the dielectric function in Refs. 13–15):

$$q_{TF} = \frac{2me^2}{\kappa\hbar^2} \quad \text{2D}, \tag{29a}$$

$$q_{TF} = \left(\frac{4me^2k_F}{\pi\kappa\hbar^2}\right)^{1/2} \quad \text{3D}, \tag{29b}$$

$$q_{TF} = \frac{4e^2k_F}{\kappa\hbar v_0} \quad \text{graphene}. \tag{29c}$$

We have used a valley degeneracy of 1 (2) for 2D/3D (graphene) systems in Eqs. (29), and chosen a spin degeneracy of 2. We note the (well-known) results that in the 2D parabolic electron system the screening wave vector is a constant, whereas in graphene (3D parabolic system) it is proportional to k_F ($\sqrt{k_F}$).

It may be worthwhile to discuss the dimensionless screening strength characterized by the parameter $q_s = q_{TF}/2k_F$, which is given by

$$q_s = \frac{2me^2}{\kappa\hbar^2k_F} \sim n^{-1/2} \quad \text{2D}, \tag{30a}$$

$$q_s = \left(\frac{4me^2}{\pi\kappa\hbar^2k_F}\right)^{1/2} \sim n^{-1/6} \quad \text{3D}, \tag{30b}$$

$$q_s = \frac{4e^2}{\kappa\hbar v_0} \sim n^0 \quad \text{graphene}. \tag{30c}$$

We note the curious (albeit well-established) result that the dimensionless screening strength increases (very slowly in 3D $\sim n^{-1/6}$) with decreasing density ($\sim n^{-1/2}$ in 2D) except in graphene where $q_{TF} \propto k_F$ leading to a density-independent q_s. Thus, the strong (weak) screening limit with $q_s = q_{TF}/2k_F \gg 1$ ($\ll 1$) is reached at low (high) carrier density in 2D and 3D metallic systems. This peculiar density-dependence of screening has qualitative repercussion for the transport exponents α and β as a function of density.

We now rewrite Eq. (8) for the 2D relaxation rate τ^{-1} in terms of screened Coulomb disorder obtaining;

$$\tau^{-1} = \left(\frac{n_i m}{\pi\hbar^3k_F^2}\right)\left(\frac{2\pi e^2}{\kappa}\right)^2 I_{22}(q_s,d_0), \tag{31}$$

with

$$I_{22}(q_s,d_0) = \int_0^1 \frac{e^{-2xd_0}x^2dx}{(x+q_s)^2\sqrt{1-x^2}}, \tag{32}$$

for 2D carriers and 2D impurities (with impurity density n_i per unit area) with $q_s = q_{TF}/2k_F$ and $d_0 = 2k_Fd$ (with $z = d$ defining the impurity locations).

$$\tau^{-1} = \left(\frac{N_i m}{8\pi\hbar^3k_F^3}\right)\left(\frac{2\pi e^2}{\kappa}\right)^2 I_{23}(q_s), \tag{33}$$

with

$$I_{23}(q_s) = \int_0^1 \frac{dx}{(q_s+\sqrt{1-x^2})^2}, \tag{34}$$

for 2D carriers and 3D impurities (with impurity density N_i per unit volume). We note that putting $q_s = 0$ (i.e. no screening) immediately produces the density scaling exponents obtained in the last subsection.

For 3D carriers with (obviously) 3D random charged impurity distribution, we get

$$\tau^{-1} = \left(\frac{N_i m}{8\pi\hbar^3k_F^3}\right) I_{33}(q_s), \tag{35}$$

where

$$I_{33}(q_s) = \int_0^1 dx \frac{1-x}{(1-x+2q_s^2)^2}. \tag{36}$$

Again, putting $q_s = 0$ in the 3D result above produces the logarithmically divergent relaxation rate discussed in Sec. IIIB for the 3D unscreened Coulomb disorder.

Finally, for graphene we write down the relaxation rates for scattering by screened Coulomb disorder arising 2D and 3D charged impurity distributions respectively by following the standard references[9,16]:

$$\tau^{-1} = \left(\frac{n_i}{\pi\hbar^2 v_0 k_F}\right)\left(\frac{2\pi e^2}{\kappa}\right)^2 I_{G2}(q_s, d_0), \tag{37}$$

where

$$I_{G2} = \int_0^1 dx \frac{x^2\sqrt{1-x^2}}{(x+q_s)^2} e^{-2xd_0}, \tag{38}$$

for 2D charged impurities located a distance d (with $d_0 = 2k_F d$) from the graphene plane, and for 3D disorder:

$$\tau^{-1} = \left(\frac{N_i}{\pi\hbar^2 v_0 k_F^2}\right)\left(\frac{2\pi e^2}{\kappa}\right)^2 I_{G3}(q_s), \tag{39}$$

with

$$I_{G3} = \int_0^1 dx \frac{x\sqrt{1-x^2}}{(x+q_s)^2}, \tag{40}$$

and N_i being the 3D impurity density. In the 3D Coulomb disorder case for graphene, the random charged impurities are distributed in the graphene substrate with a uniform random 3D distribution with a 3D impurity density of N_i.

For our numerical calculations of transport properties (to be presented in the next section) which would focus entirely on 2D systems with 2D impurities (both near and remote), we will include the realistic width of the quantum well through a subband form-factor modifying the Coulomb matrix element arising from the finite thickness of the quantum well in the z-direction. This is a nonessential complication (making our numerical results compatible with and comparable with the experimental low-temperature transport data in GaAs quantum wells) which does not affect our theoretical conclusions about the carrier density scaling of the 2D transport properties since the quasi-2D quantum well form factor is independent of the carrier density in the leading order.

Below we obtain the asymptotic density exponents (based on the results given above) α and β for screened Coulomb disorder in the strong ($q_s \gg 1$) and weak ($q_s \ll 1$) screening situations considering both near and remote 2D impurities and 3D impurities.

D. Strong-screening ($q_s \gg 1$) and weak-screening ($q_s \ll 1$) limits

It is straightforward to carry out the asymptotic expansions of the various integrals in Eqs. (31)–(40) to obtain the strong-screening ($q_s \gg 1$) and the weak-screening ($q_s \ll 1$) limiting behaviors of the relaxation rate τ^{-1} for the different systems under consideration. Remembering that $\tau^{-1} \sim n^{-\alpha}$ and $\beta = \alpha + 1$ ($\alpha + 1/2$ for graphene) we get the following results by taking $q_s \gg 1$ and $q_s \ll 1$ limits of Eqs. (31)–(40) in various situations.

(i) 2D carriers with 2D impurities:
For $2k_F d \ll 1$ (i.e. near impurities)
$\alpha = 0$ ($\beta = 1$) for strong screening ($q_{TF} \gg 2k_F$)
$\alpha = 1$ ($\beta = 2$) for weak screening ($q_{TF} \ll 2k_F$).
For $2k_F d \gg 1$ (i.e. remote impurities)
$\alpha = 3/2$ ($\beta = 5/2$) for both weak ($q_{TF} \ll 2k_F$) and strong ($q_{TF} \gg 2k_F$) screening.

(ii) 2D carriers with 3D impurities:
$\alpha = 1/2$ ($\beta = 3/2$) for strong screening ($q_{TF} \gg 2k_F$)
$\alpha = 3/2$ ($\beta = 5/2$) for weak screening ($q_{TF} \ll 2k_F$).

(iii) 3D carriers with 3D impurities:
$\alpha = 1/3$ ($\beta = 4/3$) for strong screening ($q_{TF} \gg 2k_F$)
$\alpha = 1$ ($\beta = 2$) for weak screening ($q_{TF} \ll 2k_F$).

(iv) Graphene with 2D impurities (remembering $\alpha = \alpha_\tau - 1/2 = \alpha_\mu$):
For $2k_F d \ll 1$ (i.e. near impurities) $\alpha_\tau = 1/2$; $\alpha = 0$ ($\beta = 1$) for both strong and weak screening.
For $2k_F d \gg 1$ (i.e., remote impurities) $\alpha_\tau = 1$; $\alpha = 1/2$ ($\beta = 3/2$) for both strong and weak screening.
We note that for graphene $\alpha = \alpha_\mu = \alpha_\tau - 1/2$ (and $\beta = \alpha + 1$) by virtue of its linear dispersion. Also, for graphene strongly screened, weakly screened and unscreened Coulomb disorder manifest the same density exponent in the conductivity and the mobility since $q_{TF} \propto k_F$, and thus q_s is density independent. (Of course, the actual numerical values of the conductivity and the mobility are very different in the three approximations except for having the same power law dependence on the carrier density depending only on whether the random 2D charged impurities are near or far.)

(v) Graphene with screened 3D impurities: $\alpha_\tau = 1$; $\alpha = 1/2$ ($\beta = 3/2$) for both strong and weak screening.
We note that graphene with unscreened 3D Coulomb disorder ($q_s = 0$) has the same logarithmic divergence in the relaxation rate τ^{-1} (and hence in the resistivity) for all carrier densities as in the corresponding 2D and 3D parabolic electron systems for unscreened 3D disorder. The unscreened 3D Coulomb disorder is thus unphysical, always necessitating an infra-red regularization as was already realized in the 1950s in the context of 3D doped semiconductor transport[11,12].

In Table I we summarize our asymptotic analytic findings for the density scaling of conductivity and mobility for 2D, 3D parabolic systems and 2D graphene in various limiting situations involving Coulomb disorder arising from random charged impurities in the environment.

In Table I above we provide the asymptotic density scaling exponent (α) for the carrier mobility ($\mu \sim n^\alpha$) in

		2D	3D	Graphene
2D Coulomb disorder with near impurities ($2k_Fd \ll 1$)	strong screening ($q_s \gg 1$)	0	N/A	0
	weak screening ($q_s \ll 1$)	1	N/A	0
	unscreened ($q_s = 0$)	1	N/A	0
2D Coulomb disorder with remote impurities ($2k_Fd \gg 1$)	strong screening ($q_s \gg 1$)	3/2	N/A	1/2
	weak screening ($q_s \ll 1$)	3/2	N/A	1/2
	unscreened ($q_s = 0$)	3/2	N/A	1/2
3D Coulomb disorder with 3D impurity distribution	strong screening	1/2	1/3	1/2
	weak screening	3/2	1	1/2
	unscreened	log-divergent	log-divergent	log-divergent
zero-range disorder with δ-function impurities	concept of screening inapplicable here	0	$-1/3$	-1

Table I. Asymptotic values of α. By considering the Coulomb disorder arising from random charged impurities in the environment the asymptotic density scaling exponent (α) for the carrier mobility ($\mu \sim n^\alpha$) in various limiting situations and for various types of disorder is given. The corresponding conductivity exponent (β) with $\sigma \sim n^\beta$ is given by $\beta = \alpha + 1$.

various limiting situations and for various types of disorder. The corresponding conductivity exponent (β) with $\sigma \sim n^\beta$ is given by $\beta = \alpha + 1$.

IV. RESULTS

In this section we present our numerical results for the $T = 0$ density dependent transport properties of 2D systems within the Boltzmann transport theory in order to obtain the full density dependence of the exponent $\alpha(n)$ for mobility and equivalently the exponent $\beta(n)$ for conductivity, obtaining in the process the density regimes where the analytical asymptotic exponents obtaining in the last section apply. The reason we focus on the 2D carrier system is that it is the most convenient system for the experimental investigation of the density dependence of transport properties. In 3D semiconductor systems, the carrier density cannot be continuously tuned as it can be in 2D systems.

We first note that the strong (weak) screening condition implies low (high) values of carrier density in the system. Using Eq. (11) and Eq. (29), we find: $q_s = q_{TF}/2k_F \gg 1$ implies $2me^2/\kappa\hbar^2 \gg 2(2\pi n)^{1/2}$: 2D, $(4me^2/\pi\kappa\hbar^2)^{1/2}(3\pi^2 n)^{1/6} \gg 2(3\pi^2 n)^{1/3}$: 3D, $(4e^2k_F/\kappa\hbar v_0) \gg 2k_F$: graphene, i.e.,

$$\frac{1}{8\pi}\left(\frac{2me^2}{\kappa\hbar^2}\right)^2 \gg n \quad \text{2D}, \tag{41a}$$

$$\frac{1}{2\pi^2}\left(\frac{4me^2}{\pi\kappa\hbar^2}\right)^3 \gg n \quad \text{3D}, \tag{41b}$$

$$\left(\frac{2e^2}{\kappa\hbar}\right) \gg v_0 \quad \text{graphene}. \tag{41c}$$

Eq. (41) define the low-density regime where the strong screening condition would be satisfied except for graphene which has q_s independent of carrier density since $q_{TF} \propto k_F$. From Eq. (41) we conclude that strong (weak) screening situation (within RPA) for $T = 0$ transport properties would be satisfied under the following conditions for the different systems under consideration:

$$n \ll (\gg) \left(\frac{m}{m_e\kappa}\right)^2 \times 1.14 \times 10^{16} cm^{-2} \quad \text{2D}, \tag{42a}$$

$$n \ll (\gg) \left(\frac{m}{m_e\kappa}\right)^3 \times 7.4 \times 10^{21} cm^{-2} \quad \text{3D}, \tag{42b}$$

$$\kappa \ll (\gg)\ 4.4 \quad \text{graphene}. \tag{42c}$$

Using the band effective mass for GaAs electrons ($m = 0.07m_e$) and holes ($m = 0.4m_e$), we get (using $\kappa = 13$ for GaAs-AlGaAs quantum wells)

$$n \ll (\gg)\ 3.3 \times 10^{11} cm^{-2} \ \text{for 2D n} - \text{GaAs}, \tag{43a}$$

$$n \ll (\gg)\ 9.5 \times 10^{13} cm^{-2} \ \text{for 2D p} - \text{GaAs}, \tag{43b}$$

and

$$n \ll (\gg)\ 1.5 \times 10^{15} cm^{-3} \ \text{for 3D n} - \text{GaAs}, \tag{44a}$$

$$n \ll (\gg)\ 2.8 \times 10^{17} cm^{-3} \ \text{for 3D p} - \text{GaAs}. \tag{44b}$$

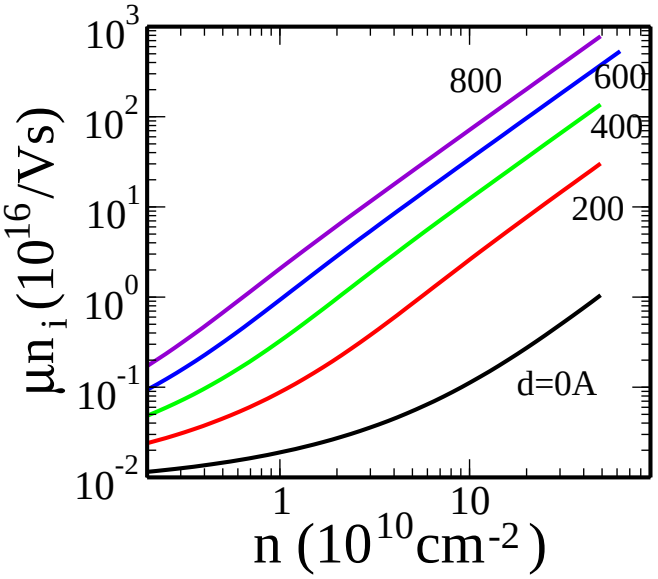

Figure 1. (color online) Calculated mobility, μn_i, as a function of density n of n-GaAs quantum well with a well width $a = 200$ Å for various d =0, 200, 400, 600, 800 Å(from bottom to top). Here n_i is the 2D random charged impurity density located a distance d away from the quantum well. The mobility is calculated at $T = 0$ K.

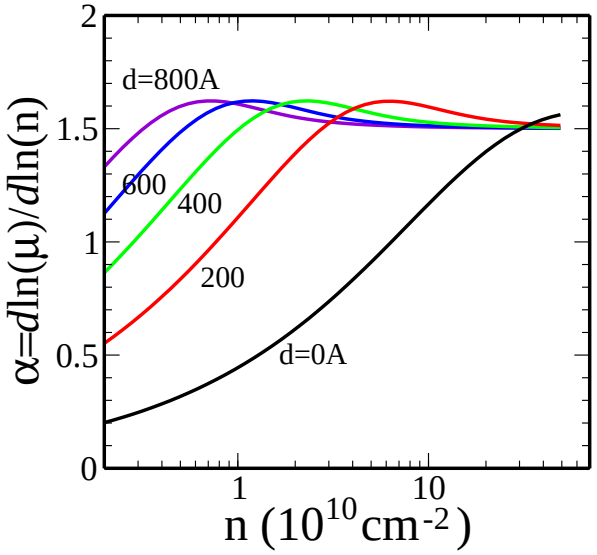

Figure 2. (color online) Calculated mobility exponent α in $\mu \propto n^{\alpha}$ (i.e., $\alpha = d\ln\mu/d\ln n$) for the corresponding $\mu(n)$ in Fig. 1.

We note (again) that in graphene (as Table I indicates) the exponents α, β do not depend on weak/strong screening or on the carrier density. The density range for GaAs-based 2D systems, which we would consider numerically in this section, is the experimentally relevant $10^9 - 10^{12}$ cm^{-2} density range in high-mobility GaAs-Al$_x$Ga$_{1-x}$As 2D quantum well structures, and thus for 2D electron systems (2D n-GaAs) the crossover from the low-density strong-screening to high-density weak-screening behavior may be experimentally relevant. On the other hand, for 2D p-GaAs hole quantum wells, the crossover density ($\sim 10^{14}$ cm^{-2}) is too high to be relevant experimentally, and thus the laboratory 2D hole systems are likely to be always in the strongly screened situation.

The 2D transport exponents α and β depend on an additional dimensionless parameter (i.e. in addition to $q_s = q_{TF}/2k_F$) $d_0 = 2k_F d$, which depends both on the carrier density through $k_F \sim \sqrt{n}$ and on the separation (d) of the random charged impurities from the 2D system. This dependence on $k_F d$, the dimensionless separation of the impurities from the carriers in the z direction (which has no analog in the corresponding 3D disordered case), is experimentally always relevant in high-mobility 2D semiconductor structures for three reasons: (1) in high-mobility modulation-doped 2D quantum well structures, scattering by remote dopants (which are introduced intentionally at a known distance d from the quantum well) is always present; (2) in principle, it is always possible to place ionized impurities at a set distance d from the 2D quantum well using the computer-controlled MBE growth technique which is used to produce high-quality semiconductor quantum wells to begin with; (3) in realistic experimental samples with a finite quasi-2D thickness, d is always finite.

In general, the experimental 2D mobility/conductivity could be limited by various types of Coulomb disorder[17]: near/far 2D Coulomb disorder ($2k_F d \ll 1/ \gg 1$): 3D Coulomb disorder in the background. According to Table I, the asymptotic density dependence in each case should be different. In Figs. 1 and 2 we show our directly numerically calculated n-2D GaAs mobility for quantum well electrons assuming 2D random charged impurity scattering from quenched point scattering centers located a distance d away from the quantum well (including the $d = 0$ case). The numerically calculated mobility exponent $\alpha(n) = d\ln\mu/d\ln n$ is shown in Fig. 2 for the corresponding $\mu(n)$ shown in Fig. 1 – we note that $n \propto k_F^2$, and therefore the parameter $k_F d \sim \sqrt{n}$ for a fixed value of d. The results shown in Figs. 1 and 2 correspond to the zero-temperature case, but are indistinguishable from the corresponding low-temperature results for $T = 300mK$ (which we have verified explicitly). We note that the numerical results presented in Figs. 1 and 2 are realistic (as are all other numerical results shown in this paper) in the sense that they are obtained from the full numerical integration of the Boltzmann theory expression for the relaxation rate [as given in Eq. (8) in section III] with the additional sophistication of including the finite thickness of the quantum well through the finite well-thickness form-factors $f_i(q)$ and $f(q)$ which modify the Coulomb disorder matrix element (i.e. $|V|^2 \to |V|^2 f_i(q)$)

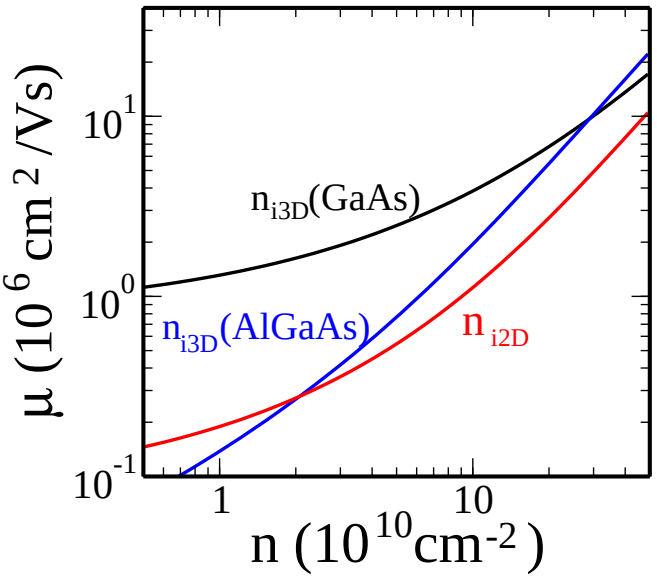

Figure 3. (color online) Calculated mobility of n-GaAs quantum well ($a = 200$Å) with unintentional charged impurities. Here the 2D impurities ($n_{i2D} = 10^9$ cm^{-2}) are at the GaAs-AlGaAs interface whereas there are two different types of 3D Coulomb disorder: inside the GaAs well [$n_{i3D} = 10^{14}$ cm^{-3} (GaAs)] and inside the barrier AlGaAs [$n_{i3D} = 10^{15}$ cm^{-3}(AlGaAs)].

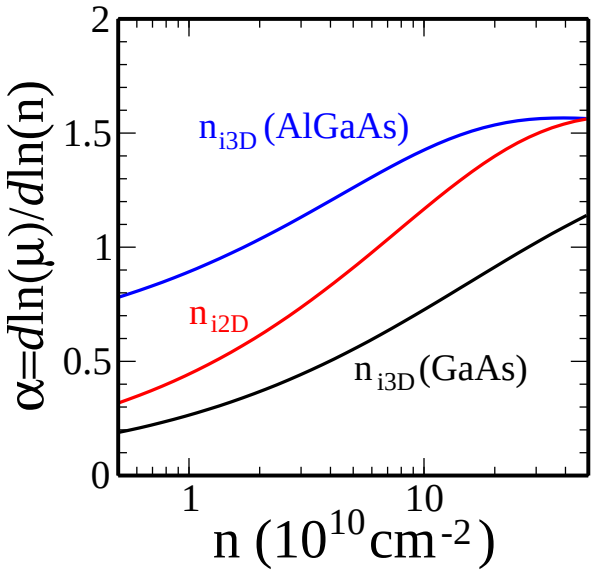

Figure 4. (color online) Calculated mobility exponent α in $\mu \propto n^{\alpha}$ (i.e., $\alpha = d\ln\mu/d\ln n$) for the corresponding $\mu(n)$ in Fig. 3.

and $q_{TF} \to q_{TF} f(q)$, respectively, and they are given by

$$f_i(q) = \frac{4}{qa}\frac{2\pi^2(1-e^{-qa/2})+(qa)^2}{4\pi^2+(qa)^2},$$
$$f(q) = \frac{3(qa)+8\pi^2/(qa)}{(qa)^2+4\pi^2} - \frac{32\pi^4[1-\exp(-qa)]}{(qa)^2[(qa)^2+4\pi^2]^2}. \quad (45)$$

where a refers to the quantum well width taken to be 200 Å for the results in Figs. 1 and 2. We note that the form-factor $f_i(q)$ simply reduces the Coulomb impurity potential from its q^{-1} behavior by a q-dependent (but density-independent) function determined by the thickness a of the GaAs quantum well. The form-factor $f(q)$ reduces the 2D screening through the modification of the electron-electron interaction due to the finite thickness of the quantum well. Since the quantum well form factors do not depend on the carrier density in the leading order, this quasi-2D form-factor effect does not in any way modify the asymptotic exponents α and β given in Table I (and theoretically defined in the lase section), but the form factors do modify the actual calculated values of the mobility/conductivity/resistivity, making them more realistic, and therefore any comparison with experimental transport data necessitates the inclusion of the quasi-2D form factor effect. All our numerical results for 2D electrons and holes in GaAs quantum wells presented in this paper include the realistic quantum well form factors in the theory taking into account the finite well width effect both in the electron-impurity interaction and in the electron screening [with q_{TF} being modified to $q_{TF} f(q)$].

In Fig. 1 we show (we actually show the calculated μn_i since $\mu \sim 1/n_i$) our calculated mobility μ for 2D n-GaAs as a function of carrier density n for different impurity locations (d) whereas in Fig. 2 we show the corresponding mobility exponent $\alpha(n) = d\ln\mu/d\ln n$. The asymptotic high-density results, $\alpha \to 3/2$ for $n \to \infty$ (i.e., $q_{TF} \ll 2k_F$) and $k_F d \gg 1$ as given in Table I, is clearly obeyed in all cases with $\alpha \approx 3/2$ for larger d and n values satisfying $2k_F d \gg 1$. For 2D GaAs systems:

$$2k_F d \approx 5\tilde{d}\sqrt{\tilde{n}}, \quad (46)$$

where $\tilde{d}$ is measured in 1000 Å units and $\tilde{n}$ in units of 10^{10} cm^{-2}. Thus even for $d = 100$Å, $2k_F d \gtrsim 1$ already for $n \gtrsim 2\times 10^{10}$ cm^{-2}, and thus the $2k_F d \gg 1$ condition is quickly reached at higher carrier density in all 2D GaAs systems for any type of relevant background 2D Coulomb disorder (since typically, $n \approx 10^9$ cm^{-2} is a lower limit for the achievable carrier density in 2D semiconductor systems). One may wonder if the $d = 0$ situation corresponds to the $2k_F d \equiv 0$ situation considered in Table I. This is certainly true for the strict 2D limit (i.e. $a = 0$ limit of the quantum well). But for any finite value of a, the $d = 0$ impurity location only refers to the distance of the 2D charged impurities from the GaAs-AlGaAs interface, and thus the average impurity separation from the electrons is always finite except in the $a \to 0$ limit. Thus even the $d = 0$ case in our theoretical calculation has an effective finite value of $d_0 = 2k_F d$ because of the finite layer thickness effect (e.g., $d \approx a/2$ effectively in the $d \to 0$ limit).

The most important conclusions from Figs. 1 and 2 are: (i) The $2k_F d \gg 1$ condition dominates the mobility exponent except for rather low mobility samples with very small values of d; (ii) even for the nominal $d = 0$ case

in Fig. 1 (where in the strict 2D case, $\alpha \lesssim 1$ always) α eventually approaches the asymptotic $\alpha \to 3/2$ value for $n \gg 10^{11}$ cm^{-2} because of the finite layer thickness effect (i.e., finite a); (iv) for scattering purely by very remote dopants ($d \gtrsim 500$ Å), the mobility exponent $\alpha > 1$ always because $2k_F d \gg 1$ condition is always satisfied; (v) the low density limit ($2k_F d \ll 1$, $q_s \gg 1$), where $\alpha \to 0$ according to Table I, would be achieved in 2D n-GaAs systems only for $n \ll 10^9$ cm^{-2}, and in all realistic situations, $\alpha > 0.5$ always as long as transport is dominated by 2D Coulomb disorder.

In Fig. 3 and 4 we show (again for $a = 200$ Å) our calculated mobility in the presence of both 2D and 3D (unintentional background) disorder neglecting remote scattering effects (assuming the intentional remote dopants to be too far, $d > 1000$ Å, for them to have any quantitative effects, as would apply to gated undoped HIGFET structures or to extreme high-mobility modulation doped structures where the intentional dopants are placed very far away). In Figs. 3 and 4, the 2D impurities (n_{i2D}) are put right at the GaAs-AlGaAs interface whereas there are two different types of 3D Coulomb disorder: inside the GaAs well [n_{i3D} (GaAs)] and inside the barrier AlGaAs [n_{i3D} (AlGaAs)]. Again the corresponding critical exponents increase with carrier density, approaching $\alpha = 3/2$ for high density consistent with the analytic theory. When the dominant background disorder is that arising from n_{i3D}(GaAs), i.e., unintentional background impurities in the well itself, typically $\alpha \approx 0.5-0.8$, which is in between weak and strong screening situation.

In Figs. 5 and 6, we show our 2D p-GaAs results for hole-doped high-mobility GaAs quantum wells. Everything in Figs. 5 and 6 is identical except for using two different hole effective mass values: $m_h = 0.3m_0$ (Fig. 5) and $0.4m_0$ (Fig.6) since the hole effective mass in GaAs quantum wells is somewhat uncertain[18]. The precise value of m_h affects $q_{TF} \propto m$, and thus determines the value of $q_s = q_{TF}/2k_F$, leading to some difference between the results in Figs. 5 and 6. For the holes, we show both the individual mobility and exponent for each scattering process as well as the total mobility and total exponent obtained by adding the two resistivities (or equivalently, the two scattering rates arising from the two scattering mechanisms). We deliberately refrain from showing the hole results (Figs. 5 and 6) in the same format as the electron results (Figs. 1 and 2) since they would all look identical except for some changes in the numbers.

In Figs. 5/6 (a) and (c) we show the calculated 2D hole mobility $\mu(n)$ limited by 3D Coulomb scattering (n_{i3D}) and 2D remote Coulomb scattering (n_i) for $a = 200$ Å with the only difference being $n_i = 8(4) \times 10^{11}$ cm^{-2} respectively in Fig. 5/6 (a) (c), showing explicitly the quantitative importance of 2D remote Coulomb scattering vis a vis 3D Coulomb scattering. The corresponding critical exponent $\alpha(n)$, shown in Fig. 5/6 (b) and (d) respectively, is completely consistent with Table I with α for remote scattering quickly reaching the asymptotic unscreened value of 3/2 as $2k_F d \gg 1$ and α for 3D Coulomb disorder increasing slowly from the very strongly screened low density situation ($\alpha_{3D} \lesssim 0.1$ for $n < 2\times 10^9$ cm^{-2}) to $\alpha \sim 1$ for very high hole density ($n \sim 10^{12}$ cm^{-2}) where screening weakens.

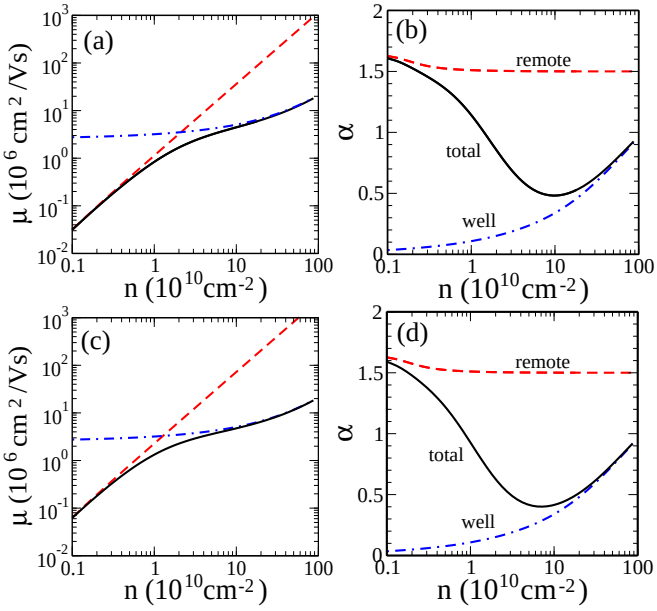

Figure 5. (color online) (a) Hole mobility as a function of hole density (n) of p-GaAs quantum well with a width $a = 200$ Å and the hole mass of $m = 0.3$. Here the background unintentional charged impurities with a density $n_{i3D} = 3 \times 10^{13} cm^{-3}$ are located inside the quantum well and 2D remote charged impurities with a density $n_i = 8 \times 10^{11} cm^{-2}$ are located at $d = 150$ Å from the interface. In this figure the black solid curve indicates the total mobility and blue dot-dashed (red dashed) curve indicates the mobility limited by only background scattering (remote charged scattering). (b) The exponents (α) for the corresponding mobilities in (a). (c) Hole mobility with the same parameters of Fig. 5(a) except the remote charged impurity density $n_i = 4 \times 10^{11} cm^{-2}$. (d) The exponents ($\alpha$) of corresponding mobilities of (c).

The total exponent in Figs. 5 and 6 shows complicated non-monotonicity as a function of carrier density since the low-density (high-density) situation is more strongly affected by remote 2D (background 3D) Coulomb scattering and the density dependent crossover between the two scattering regimes is completely nonuniversal depending precisely on the relative amounts of 2D and 3D Coulomb disorder (i.e., on n_{i3D}, n_i, and d). The only concrete statement one can make is that $\alpha(n)$ increases at low carrier density generally to a value larger than unity whereas at intermediate to high density it tends to stay below unity. Again, all of these results are completely consistent with the asymptotic exponents given in Table I (as long as various scattering mechanisms with different exponents are combined together).

So far we have discussed our numerical results of Figs. 1—6 in terms of their consistency with the theoretically analytically obtained critical exponents given

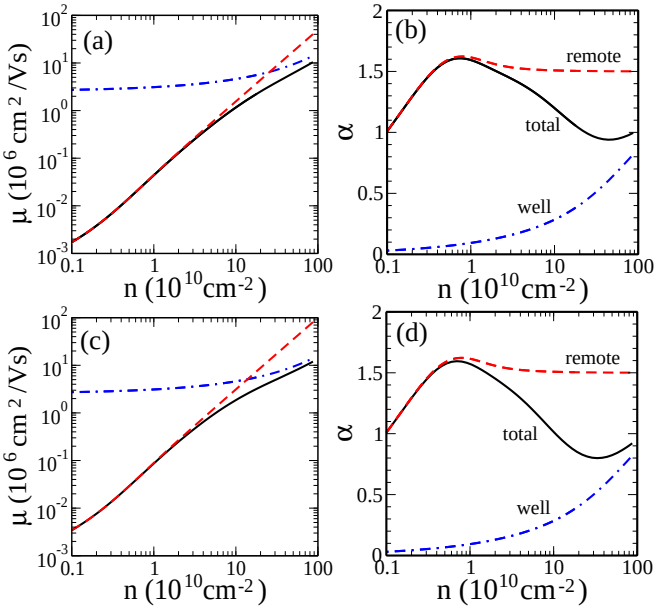

Figure 6. (color online) (a) Hole mobility as a function of hole density (n) of p-GaAs quantum well with a width a = 200 Å and the hole mass of $m = 0.4$. Here the background unintentional charged impurities with a density $n_{i3D} = 3 \times 10^{13} cm^{-3}$ are located inside the quantum well and 2D remote charged impurities with a density $n_i = 8 \times 10^{11} cm^{-2}$ are located at d = 800 Å from the interface. In this figure the black solid curve indicates the total mobility and blue dot-dashed (red dashed) curve indicates the mobility limited by only background scattering (remote charged scattering). (b) The exponents (α) for the corresponding mobilities in (a). (c) Hole mobility with the same parameters of Fig. 5(a) except the remote charged impurity density $n_i = 4 \times 10^{11} cm^{-2}$. (d) The exponents ($\alpha$) of corresponding mobilities of (c).

in Table I with the mobility exponent ($\mu \sim n^{\alpha(n)}$) α showing the expected behavior in the asymptotic density regimes of $2k_Fd \gg 1$ ($\ll 1$) and $q_s \gg 1$ ($\ll 1$) as the case may be. Remote scattering by 2D ionized dopants dominates transport at low density ($2k_Fd < 1$) crossing over to background impurity scattering dominated regime at higher density, leading to $\alpha > 1$ (< 1) at low (high) density.

Now we discuss perhaps the most interesting aspect of our numerical results in Figs. 1—6, which appears to be at odds with our asymptotic theoretical analysis of section III (and table I). This is the intriguing result that $\alpha(n)$ due to remote 2D impurity scattering can actually exceed the asymptotic unscreened 2D Coulomb scattering value of $\alpha = 3/2$. It is clear in Figs. 2, 4, 5(b), 5(d), 6(b), 6(d) that there is a shallow maximum in $\alpha(n)$ at some intermediate density where the numerically calculated mobility exponent $\alpha > 3/2 = 1.5$ (and therefore the corresponding conductivity exponent $\beta > 2.5$), which is remarkable since the unscreened Coulomb scattering (applicable in the high-density regime defined by $2k_Fd \gg 1$ and/or $q_s \gg 1$) by remote impurities produces $\alpha = 3/2$. This non-monotonic behavior of the exponent $\alpha(n)$ in the intermediate density regime (neither high- nor low-density asymptotic regime considered in Table I) with an exponent value larger than the corresponding unscreened Coulomb exponent 3/2 is unexpected and highly intriguing. We provide a theoretical explanation for this intriguing nonmonotonic behavior of remote Coulomb scattering at intermediately density with a mobility exponent exceeding the unscreened value of 1.5 in the next section.

Before concluding this section on numerical results, we provide, for the sake of completeness, our numerically calculated mobility exponent for 2D graphene transport under the remote Coulomb scattering situation. In Fig. 7 we show our calculated graphene mobility exponent $\alpha(n)$ obtained from the numerically calculated graphene mobility, $\alpha(n) = d \ln \mu / d \ln n$, for various locations (d) of the 2D impurity layer in relation to the 2D graphene layer. We note that graphene is a strictly 2D system and hence there is no quasi-2D form factor correction. It is clear that $\alpha(n)$ goes asymptotically to the unscreened Coulomb value of 3/2 as n (and therefore k_Fd increases) except for the trivial $d = 0$ case where $\alpha(n) = 0$ (i.e., $\beta = 1$) for all density as is already well-known in the literature[9,16] and is well-verified experimentally[19].

The calculated graphene mobility exponent $\alpha(n)$ shown in Fig. 7 agrees completely with the analytical exponent values given in Table I. (We mention again that in graphene the mobility exponent $\alpha_\mu = \alpha$ and the relaxation rate exponent α_τ differ with $\alpha = \alpha_\mu = \alpha_\tau - 1/2$ and $\beta = \alpha + 1 = \alpha_\mu + 1$ by definition whereas in 2D and 3D parabolic system, where $\mu \propto \tau$, $\alpha_\mu = \alpha_\tau = \alpha = \beta - 1$.) We note that in graphene, for impurities away from the 2D graphene plane (i.e., $d \neq 0$), the asymptotic conductivity exponent β for high carrier densities ($k_Fd \gg 1$) is 3/2 and thus $\sigma \propto n^{3/2}$ in graphene layers dominated by far away Coulomb impurities. An experimental verification of such a $\sigma \sim n^{3/2}$ behavior in graphene due to Coulomb scattering by remote impurities will be a direct verification of our theory.

V. NONMONOTONICITY OF TRANSPORT SCALING

We now theoretically discuss (and explain analytically) our surprising numerical finding in section IV, not anticipated at all in the asymptotic theory of section II or in any of the substantial earlier literature on 2D transport, that the density scaling exponent α (β) of 2D mobility (conductivity) has an intriguing nonmonotonicity as a function of carrier density in the intermediate density regime (in-between the asymptotic low and high density regimes discussed in section III and tabulated in Table I).

We first note that the nonmonotonicity in $\alpha(n)$ arises from the subtle fact that although the exponent α (or β) depends only on one explicit external variable (namely, the carrier density n), it depends theoretically on two

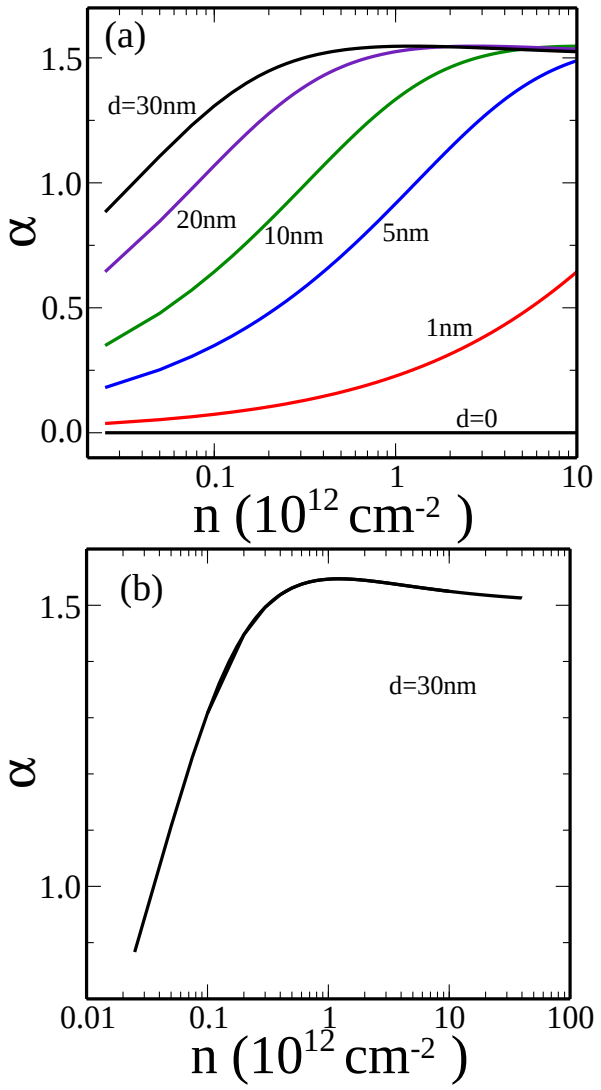

Figure 7. (color online) (a) shows the calculated graphene mobility exponent $\alpha(n)$ obtained from the numerically calculated graphene mobility, $\alpha(n) = d\ln\mu/d\ln n$, for various location ($d$) of the 2D impurity layer in relation to the 2D graphene layer. In (b) the exponent for $d = 30$ nm shows a shallow local maximum at $n \sim 10^{12}$ cm^{-2}.

independent dimensionless variables $q_s = q_{TF}/2k_F$ and $d_0 = 2k_F d$ since in reality there are two independent external variables in the problem: carrier density (n) and the impurity location (d). The dependence on two independent variables is the key feature allowing for the presence of nonmonotonicity in $\alpha(n)$ as well as its maximum possible value being larger than the unscreened exponent value $\alpha \to 3/2$. Indeed in the strict 2D limit with $d = 0$ (see, e.g., the graphene result in Fig. 7), there is no maximum allowed in $\alpha(n)$. This is true for both graphene and 2D parabolic system – in graphene, $\alpha(n) = 0$ for all values of n in the $d = 0$ limit whereas in strictly 2D parabolic system $\alpha(n)$ monotonically increases from $\alpha = 0$ in the low-density limit ($q_s \gg 1$) to precisely $\alpha = 1$ in the high density ($q_s \ll 1$) for $d = 0$ as one would expect theoretically (we have verified this strict 2D limit with $d = 0$ result explicitly numerically).

For $d \neq 0$ (i.e., $2k_F d \neq 0$), however, the behavior of transport properties depends nontrivially on the variable $d_0 = 2k_F d$, and there is no obvious theoretical reason why the low-density ($\alpha = 0$ or 1 depending on strong or weak screening) and the high-density ($\alpha = 3/2$ always) asymptotic limits must be the lower and upper bounds on the exponent. In fact, as our numerics show, and we establish theoretically below, $\alpha(n)$ does have a peak (exceeding the unscreened $\alpha = 3/2$ value) at an intermediate density around $2k_F d \approx 1$.

As shown in our numerical results presented in the last section, $\alpha(n)$ defined by $\mu \sim n^{\alpha(n)}$, can exceed the unscreened exponent value $\alpha = 3/2$ reached in the asymptotic high-density ($2k_F d \gg 1$) limit. To verify whether this finding is a numerical artifact or real, it is sufficient to consider the unscreened remote 2D Coulomb disorder in the strict 2D electron layer limit where the free carriers and the charged impurities, both confined in infinite zero-thickness 2D layers in the x-y plane, are separated by a distance d in the z-direction. (This is the model explicitly used in section III.) As $n \to 0$, $\alpha(n) \to 1$ (unscreened $2k_F d \ll 1$ limit) whereas as $n \to \infty$, $\alpha(n) \to 3/2$ (unscreened $2k_F d \gg 1$ limit). The zero-density limit would be modified to $\alpha = 0$ if screening is included in the theory, but we are interested here in the intermediate-density behavior, not the zero-density regime.

The scattering rate τ^{-1} in this case is given by [see Eqs. (31) and (32)]:

$$\tau^{-1} = \frac{C}{n}\int_0^1 \frac{e^{-bx\sqrt{n}}}{\sqrt{1-x^2}}dx, \tag{47}$$

where we have shown the explicit density (n)-dependence everywhere (C and b are unimportant carrier density independent constants for our purpose) and have used the fact that $k_F \sim \sqrt{n}$. We rewrite Eq. (47) as,

$$\tau^{-1} = \frac{C}{n} I(n), \tag{48}$$

where

$$I(n) = \int_0^1 \frac{e^{-bx\sqrt{n}}}{\sqrt{1-x^2}}dx. \tag{49}$$

It is obvious that τ^{-1} is a monotonic function of n decreasing continuously with increasing density with no extrema whatsoever since both $1/n$ and $\exp(-bx\sqrt{n})$ decrease with increasing n continuously. This can be easily checked explicitly by showing that the equation $d\tau^{-1}(n)/dn = 0$ has no solution. The monotonic decrease of $\tau^{-1}(n)$ with n simply implies that $\mu(n) \propto \tau(n)$ increases monotonically with increasing density as is obvious from our numerical results in section IV: For Coulomb disorder, 2D mobility and conductivity always increase with increasing density monotonically.

To figure out whether $\alpha(n) = d\ln\mu/d\ln n$ has non-monotonicity (or extrema) as a function of n, we must use $\mu(n) \propto \tau(n)$, and write

$$\alpha = \frac{d\ln\mu}{d\ln n} = n\frac{d\ln\mu}{dn} = 1 - \frac{n}{I}\frac{dI}{dn}, \tag{50}$$

where $I(n)$ is the integral defined by Eq. (49). It is straightforward, but messy, to show that the condition $d\mu/dn = 0$ with $\alpha(n)$ defined by Eq. (50) has a solution at an intermediate value of n, and thus $\alpha(n)$ has an extremum – it is still messier to show that $d^2\alpha/dn^2 < 0$ at this extremum so that $\alpha(n)$ has a maximum at an intermediate density as is found numerically in section IV. For our purpose, however, it is much easier to simply establish that the function $\alpha(n)$ defined by Eq. (50) approaches the high density $n \to \infty$ limit of $\alpha(n \to \infty) = 3/2$ from above, thus definitively proving that the mobility exponent α exceeds $3/2$ at some intermediate density (and thus must have a maximum in the $0 < n < \infty$ or equivalently in the $1 \gg k_F d \gg 1$ regime).

As $n \to 0$, we have from Eq. (49):

$$I(n) = \pi - b\sqrt{n}, \tag{51}$$

leading to

$$\alpha(n \to 0) = 1 + b\sqrt{n}/\pi. \tag{52}$$

As $n \to \infty$, we have:

$$I(n) = \frac{1}{b\sqrt{n}}\left[1 + \frac{1}{b^2 n}\right], \tag{53}$$

leading to

$$\alpha(n \to \infty) = 3/2 + 1/2b^2 n. \tag{54}$$

From Eqs. (31), (32), (47), and (48) we have: $b = 2\sqrt{2\pi}d$, and thus $b \propto d$ is positive definite (except for the $d = 0$ explicitly left out here). We, therefore, immediately conclude that $\alpha(n)$ approaches its asymptotic value of $\alpha = 3/2$ for $n \to \infty$ from above with $\alpha(n \to \infty) \approx \frac{3}{2} + \frac{1}{16\pi d^2}\frac{1}{n}$, and the leading possible correction to the exponent in the $n \to \infty$ limit is of $O(1/n)$ with a coefficient $1/16\pi d^2 \propto d^{-2}$. We also find that the correction to the $n \to 0$ value of $\alpha(n = 0) = 1$ is of $O(\sqrt{n})$ with a positive coefficient of $2\sqrt{2\pi}d/\pi \propto d$. Thus, we now have a complete theoretical understanding of the intriguing (and hitherto unexpected in the literature) numerical finding in Sec. IV that, although the mobility $\mu(n)$ itself is a monotonically increasing function of increasing carrier density, its power law exponent $\alpha(n)$ shows a maximum (around $2k_F d \sim 1$ in fact) approaching the asymptotic high-density ($n \to \infty$; $2k_F d \gg 1$) value of $\alpha = 3/2$ from above, allowing $\alpha(n)$ to be larger than 1.5 at some d-dependent value $\alpha > 1.5$.

One feature of our theory presented in Eqs. (47) – (54) is worth mentioning and comparing with the numerical results of Sec. IV. This is our finding in Eq. (54) that the asymptotic high-density ($n \to \infty$) exponent $\alpha(n \to \infty) = 3/2$ is approached from above as $\alpha(n \to \infty) = 3/2 + 1/(16\pi d^2 n)$, implying that the maximum possible values of α, $\alpha_{\max}$, scales approximately as $(d^2 n_{\max})^{-1} \propto (k_{Fm} d)^2$, where $n_{\max}$ and k_{Fm} are respectively the carrier density and the corresponding Fermi wave vector at the maximum. This implies that the maximum value $\alpha_{\max} \approx 1.7$ ($\approx 3/2 + 1/16\pi$) is approximately independent of the value d and of the carrier effective mass with the value of the carrier density $n_{\max}$ (where the maximum occurs) scaling roughly as $n_{\max} \sim d^{-2}$. This strong prediction is approximately consistent with our numerical results – in fact, $\alpha_{\max} \sim 1.7$ is clearly independent of whether the system is a 2D electron or hole system and of the precise value of d. In fact, $\alpha_{\max} \sim 1.7$ being approximately independent of electrons/holes and the value of the separation distance d is a striking theoretical result which is consistent with the full numerical results of Sec. IV.

Because of the striking nature of our finding that $\alpha_{\max} \sim 1.7$ always (for remote impurity scattering) for 2D electron/hole carrier systems, we carried out additional numerical calculations using the realistic Boltzmann theory (including both quasi-2D finite thickness and screening effects) for 2D n-GaAs wells of thickness $a = 300$ Å (different from the case of $a = 200$ Å used in Sec. IV) and incorporating both remote impurity scattering with 2D impurity densities n_d and separation d and also (different values of n_d is used) with near impurity scattering with 2D impurity density n_i with $d = 0$ (i.e. interface impurities). The calculated exponents for the individual scattering mechanisms α_d and α_i (for n_d and n_i, respectively) are shown in Fig. 8 where each panel corresponds to different sets of values for n_d and a fixed n_i. In each case, the individual exponents α_d/α_i as well as the total exponent α are shown as a function of density. The exponent is extracted from a full numerical evaluation of $\mu(n)$ and then using $\alpha(n) = d\ln\mu(n)/d\ln n$, where the total exponent is extracted by adding the two individual resistivities, i.e., $\mu^{-1} = \mu_d^{-1} + \mu_i^{-1}$. The rather amazing fact to note in Fig. 8 is that each individual exponent α_d and α_i has a maximum value ~ 1.7, albeit the maximum for remote (near) impurities occurring at low (high) carrier densities because the effective d-values are much higher (lower) for remote (near) impurities. (We note that $d = 0$ for n_i impurities still has an effective d value of roughly $a/2 \approx 150$ Å whereas the effective d for the n_d impurities is $d + a/2$ in each case.) Figure 8 is a striking direct numerical verification of our theory.

Before discussing the same physics for graphene, which we do next, we mention that including screening in the theory is straightforward (but extremely messy). All we need to do is to modify Eq. (49) to

$$I(n) = \int_0^1 \frac{x^2 e^{-bx\sqrt{n}} dx}{(x + c/\sqrt{n})^2\sqrt{1 - x^2}}, \tag{55}$$

with $c = 0$ giving the unscreened formula of Eq. (47). Inclusion of screening strongly affects the low-density

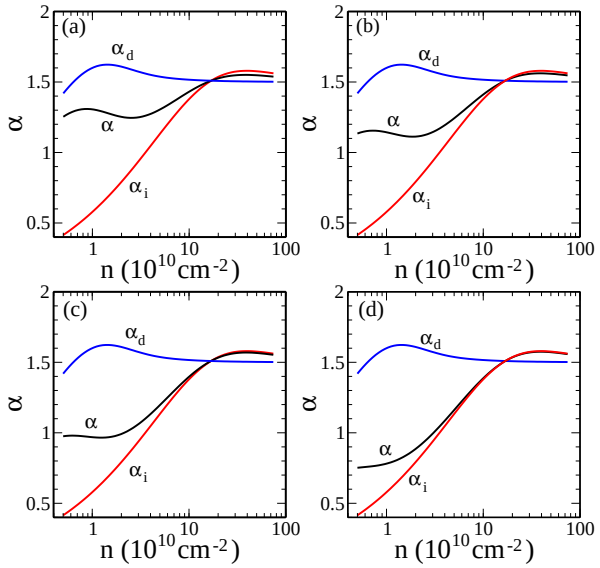

Figure 8. (color online) The calculated mobility exponent as a function of density for 2D n-GaAs wells of thickness $a = 300$ Å. The mobility is calculated by incorporating both remote impurity scattering with 2D impurity densities n_d and separation d and near impurity scattering with 2D impurity density n_i. Here we use $d = 500$ Å and $n_i = 3 \times 10^8$ cm^{-2} for all figures, but different values of n_d, i.e., (a) $n_d = 2 \times 10^{10}$ cm^{-2}, (b) $n_d = 1 \times 10^{10}$ cm^{-2}, (c) $n_d = 0.5 \times 10^{10}$ cm^{-2}, (a) $n_d = 0.22 \times 10^{10}$ cm^{-2}. The calculated exponents for the individual scattering mechanisms α_d and α_i (for n_d and n_i, respectively) and the total exponent α are shown as a function of density.

$n \to 0$ behavior, changing $\alpha(n \to 0)$ exponent to zero (for $c \neq 0$) from unity ($c = 0$), but does not affect the intermediate or high density behavior at all (as is obvious from Table I where the $2k_F d \gg 1$ asymptotic results are independent of the screening constant $q_s = q_{TF}/2k_F \propto 1/\sqrt{n}$). Since the extrema behavior of interest to us is not a low-density phenomenon, our analysis based on Eq. (49) is appropriate (as is verified by its agreement with the full numerical results).

Now, we consider the corresponding graphene case, which also has a maximum in $\alpha(n)$ at some intermediate carrier density with $\alpha_{\max}$ (> 1.5) being larger than the corresponding infinite density unscreened exponent value of 3/2 (see Fig. 7). For graphene, with the charged impurities located in a 2D layer a distance d from the graphene layer, the scattering rate τ^{-1} is given by [see Eq.(38)]:

$$\tau^{-1} = A\sqrt{n}\int_0^1 dx \frac{x^2\sqrt{1-x^2}}{(x+q_s)^2} e^{-\tilde{b}x\sqrt{n}}, \qquad (56)$$

where A, $\tilde{b} = 2\sqrt{\pi}d$ are density-independent constants and $q_s = 4e^2/\kappa\hbar v_0$ is also density independent. Direct expansion for Eq. (56) in the low ($n \to 0$) and high ($n \to \infty$) limits give:

$$\tau^{-1}(n \to 0) = \frac{A_0}{\sqrt{n}}\left(1 - \frac{16d}{3\pi}\sqrt{\pi n}\right), \qquad (57)$$

and

$$\tau^{-1}(n \to \infty) = \frac{A_\infty d}{(k_F d)^2 (q_{TF} d)^2}\left(1 - \frac{6}{q_{TF} d}\right), \qquad (58)$$

where A_0 and A_∞ are constants independent of n and d. For graphene $\mu(n) \sim \tau/\sqrt{n}$, and therefore, we get for $n \to 0$

$$\mu(n) \sim \left(1 + \frac{16d}{3\pi}\sqrt{n}\right), \qquad (59)$$

and for $n \to \infty$

$$\mu(n) \sim n^{3/2} d^3 \left(1 + \frac{3}{2r_s d\sqrt{\pi n}}\right), \qquad (60)$$

where $r_s = e^2/(\kappa\hbar v_0)$ is the so-called graphene fine structure constant.

Eqs. (56) – (60) imply that the mobility $\mu(n)$ starts at low density ($n \to 0$) with $\alpha = 0$, but with a leading order correction going as $O(\sqrt{n})$ with a positive sign. For large n (i.e., $k_F d \gg 1$), $\alpha(n \to \infty)$ becomes 3/2, but has a positive leading order correction of $O(1/\sqrt{n})$. This immediately implies that $\alpha(n)$ must have a local maximum at some intermediate density with α being only logarithmically larger than the asymptotic ($n \to \infty$) value of 3/2. This conclusion is consistent with numerical results presented in Fig. 7. We note that the maximum in $\alpha(n)$ for graphene is much shallower and weaker than in the 2D parabolic system.

VI. EXPERIMENTAL IMPLICATIONS

We now discuss the possible experimental relevance of our theoretical findings in this section. The fact that the mobility $\mu(n)$ or the conductivity $\sigma(n) = ne\mu$ of 2D carrier systems shows a density scaling behavior with $\mu \sim n^{\alpha(n)}$ and $\sigma \sim n^{\beta(n)}$ with $\beta = \alpha + 1$ has been known for a long time in the experimental 2D transport literature[10]. Although our current work is purely theoretical, focusing entirely on the fundamental questions of principle involving the detailed behavior of the exponent $\alpha(n)$ and $\beta = \alpha + 1$ for various types of disorder affecting transport properties, we believe that it is appropriate for us to comment on experiments, making connection with the existing data in the literature as well as making some concrete predictions for future experiments (particularly in the context of our unexpected finding of a maximum in $\alpha(n)$ with an almost universal value of 1.7 for 2D semiconductor quantum wells).

We first summarize the serious difficulties in making direct quantitative connection or comparison between experiment and theory in 2D semiconductor systems with respect to low-temperature disorder-limited

transport properties. In fact, these caveats apply to all disorder-limited transport properties in all systems, not just to 2D transport in semiconductor quantum wells. The key problem is that the detailed nature of disorder (either qualitative or quantitative) in a sample is never precisely known from independent measurements — in the context of our transport theory in this paper, relative amounts of 2D near and remote Coulomb disorder, 3D Coulomb disorder, and short-range disorder are simply not known. Thus, a quantitative or even a qualitative theory for calculating the mobility or the conductivity of a given sample exists only as a matter of principle, but not in practice since the details of the underlying disorder contributing to resistive scattering are apriorie unknown and often are figured out indirectly based on quantitative comparisons between transport experiment and theory. The situation is worsened by the fact that the relative magnitudes of various independent scattering mechanisms vary strongly with carrier density – for example, Coulomb disorder weakens with increasing carrier density making short-range scattering relatively stronger at high carrier density. Thus, all 2D semiconductor transport would eventually be dominated by short-range scattering (e.g., interface roughness, alloy disorder) at very high carrier density (where $\alpha \approx 0$ in 2D systems), and the only question is how high in density one must go to reach this asymptotic zero-range disorder limited regime where Coulomb disorder has virtually been screened out. This, of course, is completely nonuniversal and depends entirely on the relative amount of Coulomb impurities and short-range disorder in particular samples! This discussion shows that in 2D semiconductor we have $\alpha(n \to 0) = 0$ and $\alpha(n \to \infty) = 0$ purely theoretically with the zero-density limit and the infinite-density limit being dominated by completely screened Coulomb disorder ($k_F d \ll 1$, $q_s \gg 1$) and zero-range disorder, respectively, although these strict theoretical limits are unlikely to apply to real samples at any finite carrier density.

The difficulty of applying the pristine theory to specific experimental situations is obvious from our numerical results presented in Figs. 5 and 6 (for 2D holes) and Fig. 8 (for 2D electrons). In each case, the mobility exponent α for individual near and far Coulomb impurities follows our theoretical prescription perfectly with the expected low- and high-density exponents agreeing with the results of Table I, but the total exponent α (which is the only one relevant for the experimental data) may not follow any well-defined pattern and could vary strongly depending on the relative strengths of near and far Coulomb disorder, showing strong nonmonotonicity (Figs. 5 and 6) or weak/no nonmonotonicity (Fig. 8). This reinforces the point made earlier by us that the universal density scaling behavior in transport applies only to individual scattering mechanism with the overall transport being dominated by crossover behavior is generically nonuniversal due to the existence of several different operational scattering processes.

In spite of the above serious caveats arising from our ignorance about the underlying disorder contributing to resistive scattering mechanisms, some general statements can be made about the implications of our theory to experimental data. We discuss this below.

(i) For very dirty (and low-mobility) samples, the background Coulomb disorder arising from the unintentional charged impurities in the quantum well should dominate transport properties, leading to $\alpha_e \sim \alpha_h \sim 0.5$ for a wide range of intermediate densities. (ii) When transport is limited by remote dopants, which would always be true in modulation-doped samples for $k_F d < 1$, $\alpha_e \sim 1.5$ and $\alpha_h \sim 1 - 1.5$ depending on the hole effective mass, but α_e/α_h will decrease with increasing density as $k_F d > 1$ regime is reached. (iii) For modulation doped structures with $k_F d \gg 1$, background disorder again dominates at intermediate density giving $\alpha_e \sim \alpha_h \sim 0.5 - 1$.

The above situation seems to describe the existing experimental situation for 2D quantum well transport reasonably well as discussed below. Focusing on specific experimental results in the literature in the context of our transport theory, we make the following remarks discussing some specific experimental publications in 2D GaAs based electron and hole systems.

(1) In Ref.20, the measured $\alpha_e \approx 0.6 - 0.7$ in n-GaAs 2D system with no intentional remote dopants (the sample is a gated undoped sample) in the density range $\sim 10^{10} - 10^{11}$ cm^{-2} (i.e., $q_s \gtrsim 1$; $2k_F d < 1$) agrees quantitatively with our theoretical results given in Figs. 3, 4, and 8 with background 2D and 3D unintentional charged impurities being the main disorder mechanism as expected for an undoped 2D system.

(2) In a similar gated undoped 2D p-GaAs sample Manfra *et al.*[21] find $\alpha_h \sim 0.7$ for density $\gtrsim 10^{10}$ cm^{-2}, again agreeing with our results given in Figs. 3 and 4 for background scattering.

(3) In Harrell *et al.*[22] gated undoped n-GaAs 2D samples, $\alpha \approx 0.6$ was found for $n \gtrsim 10^{11}$ cm^{-2} and $\alpha \approx 0.33$ was found for $n < 5 \times 10^{10}$ cm^{-2}. This is both quantitatively and qualitatively consistent with our numerical findings in Figs. 3, 4, and 8, where scattering by background charged impurities in the layer leads to $\alpha \approx 0.3 - 0.7$ in the $n = 10^{10} - 10^{11}$ cm^{-2} density range with $\alpha(n)$ decreasing with decreasing carrier density.

(4) Melloch *et al.*[23] found $\alpha \approx 0.6 - 0.7$ for $n > 10^{11}$ cm^{-2} which is consistent with our background impurity scattering results.

(5) Pfeiffer *et al.* studied[24] modulation-doped high-mobility 2D GaAs electron systems[24] obtaining $\alpha \sim 0.7$ around $n \sim 3 \times 10^{11}$ cm^{-2} for modulation-doped structures ($d = 1000 - 2000$Å) with $\mu \gtrsim 10^7$ cm^2/Vs. Again, remote impurity scattering is completely ineffective here because $k_F d \gg 1$ rendering mobility limited only by remote impurity scattering to be around 10^8 cm^2/Vs according to our numerical calculations. The dominant scattering mechanism in this sample is by background unintentional charged impurities, leading to $\alpha \approx 0.7$ around $n \sim 3 \times 10^{11}$ cm^{-2} according to our Fig. 4, which is in

precise agreement with the date of Pfeiffer *et al.*[24].

(6) In a similar high-mobility modulation-doped 2D n-GaAs sample, Shayegan *et al.*[25] found $\alpha \approx 0.6$ in samples with $\mu \approx 10^6$ cm^2/Vs for $n \lesssim 10^{11}$ cm^{-2} with the spacer thickness $d = 1000-2000$ Å. Again, remote scattering by the intentional dopants is ineffective as a resistive scattering mechanism here with the dominant scattering being by unintentional background impurities in the GaAs quantum well.From Fig. 4 of our presented results, we find $\alpha \approx 0.6$ for $n \lesssim 10^{11}$ cm^{-2} in agreement with the experimental finding of Shayegan *et al.*[25].

(7) Most of the high-mobility experimental samples discussed above are dominated by the background unintentional charged impurities in the 2D layer itself leading to $\alpha < 1$ by virtue of the fact that the intentional dopants introduced for modulation doping are rather far away in these high quality samples (this is a generic feature of all high mobility 2D samples with $\mu > 10^6$ cm^2/Vs where $\alpha < 1$ prevails by virtue of the background disorder being dominant). By contrast, early work on modulation-doped 2D samples invariably had lower values of d and achieved much lower mobility $\mu < 10^6$ cm^2/Vs. Such samples are almost always dominated by remote scattering by the intentionally introduced dopants, leading to α values typically exceeding unity as our theory predicts. As a typical example, we consider the work of Hirakawa and Sakaki[26] on modulation-doped 2D n-GaAs samples with $\mu \sim 10^4 - 5\times10^5$ cm^2/Vs for $d \approx 0-180$ Å in the $n \approx 10^{11} - 5\times10^{11}$ cm^{-2} density range. Assuming transport to be limited entirely by the intentional ionized dopants in the modulation layer (i.e., no background disorder scattering), our results of Fig. 1 predict $\alpha \approx 1$ for $d = 0$ and $\alpha \approx 1.1-1.3$ for $d = 100$ Å. Hirakawa and Sakaki reported[26] $\alpha \approx 1.1-1.3$ for $d \approx 0-100$ Å in essential agreement with our theory. In addition, these authors reported $\alpha \approx 1.7$ for $d \approx 200$ Å, an anomalous mobility exponent (i.e. $d > 3/2$) which has remained unexpected in the literature for more than 25 years. Our current work provide a definitive explanation for $\alpha \approx 1.7$ as arising from the maximum in $\alpha(n)$ for remote scattering as is apparent in Fig. 1. We note that $k_F d \sim 1-2$ for $n \sim 10^{11}$ cm^{-2} and $d \sim 100-200$ Å, and thus our theory predicts $\alpha \sim 1.7$ for $d \approx 200$ Å in the Hirakawa-Sakaki experiment[26]. We believe that the experimental finding of $\alpha \sim 1.7$ by Hirakawa and Sakaki is a direct verification of our intriguing prediction of $\alpha > 3/2$ for $k_F d \gtrsim 1$ in transport dominated by remote scattering.

(8) Finally, we discuss some recent unpublished experimental work by Pfeiffer and West[27] who, motivated by our theoretical work, carried out low-temperature transport measurements in a series of high-quality (i.e. ultrapure GaAs with very little background disorder due to unintentional impurities) MBE-grown 2D n-GaAs samples with variable values of d. Since these experiments were performed with the specific goal of checking our low-temperature 2D transport theory predictions, Pfeiffer and West made undoped gated samples of highest quality with little background disorder and a nominal low-temperature mobility of $\mu > 10^7$ cm^2/Vs. Then, they systematically introduced charged impurities at specific separation (d) from the 2D layer by inserting carbon atoms in the GaAs layer ($d = 0$) or in AlGaAs barrier layer ($d \neq 0$). First they explicitly verified that the introduction of different amounts of impurity centers without changing d only affects the 2D mobility through the expected $n_i\mu$ scaling behavior (i.e. $\mu \propto n_i^{-1}$) without changing $\alpha(n)$ by changing the inserted carbon atoms by a factor 5 keeping d fixed (which changed the 2D mobility by a factor of 5 without changing the exponent $\alpha(n)$ in the same carrier density range). Thus, they measured $\alpha(n)$ for $d = 0$ and $d = 150$ Å finding $\alpha(n) \approx 0.8$ and 1.8 respectively for $n \sim 10^{11}$ cm^{-2}. Our calculated $\alpha(n \approx 10^{11}$ cm$^{-2}) \approx 0.8$ for $d = 0$ in Fig. 2 in perfect agreement with the experimental data. For $d = 150$ Å, $k_F d \approx 1$ for $n \approx 10^{11}$ cm^{-2}, and we predict $\alpha(n) \approx \alpha_{\max} = 1.7$ in this situation which compares well with the experimental exponent of 1.8. Thus, this experimental investigation of our theoretical predictions appears to have strikingly verified our finding that $\alpha > 3/2$ in the $k_F d \sim 1$ intermediate density regime where the shallow maximum occurs in $\alpha(n)$ in our theory.

(9) Before concluding our discussion of experimental implications of our theory we describe the very recent 2D hole transport data in high-mobility p-GaAs systems by the Manfra group[28,29]. These 2D p-GaAs samples with hole mobility $> 2\times10^6$ cm^2/Vs are the world's highest mobility hole samples ever, and taking into account the effective mass difference ($\sim$ a factor of 5) between GaAs electrons and holes compare favorably with the best ($\sim 15\times10^6$ cm^2/Vs) available 2D electron mobilities. The main finding of the work[28] is that the mobility exponent $\alpha(n)$ increases from 0.7 at high hole density ($\sim 10^{11}$ cm$^-2$) to 1.7 at low density ($\gtrsim 10^{10}$ cm^{-2}) for modulation doped sample with $d = 800$ Å. Since the mobility remains high throughout ($\gg 10^5$ cm^2/Vs), localization effects should not be playing a role. We therefore believe that the experimental finding of Watson *et al.*[28] is a direct confirmation of the $\alpha(n)$ behavior for 2D holes presented in our Figs. 5 and 6, where the total calculated $\alpha(n)$ increases monotonically as the 2D hole density decreases from $n \sim 10^{11}$ cm^{-2} to $n \sim 10^{10}$ cm^{-2}. In fact, even the explicit α-values measured by Watson *et al.* agree well with our 2D hole theoretical results presented in Figs. 5 and 6 with α ($n \sim 10^{10}$ cm^{-2}) increasing above the unscreened $\alpha = 3/2$ value reaching essentially the measured value of $\alpha \sim 1.7$ around $n \gtrsim 10^{10}$ cm^{-2}. Thus, our theory provides a qualitative explanation of the Watson *et al.* experimental results including the surprising finding of the intermediate-density α being around 1.7 (> 1.5).

(10) We conclude this section on the experimental relevance of our theory by discussing graphene briefly. There has been substantial research activity on studying the density dependent graphene conductivity[9,30] which is well beyond the scope of our current work and has already been covered elsewhere. It is known that scattering by near random charged impurities located on the surface

of the graphene layer or at the graphene-substrate interface leads to a $\sigma(n) \propto n$ (i.e., $\mu(n) \sim$ constant) in the intermediate density ($k_F d < 1$) region, and in the high-density regime $\sigma(n)$ becomes sublinear most likely because of short-range defect scattering which gives $\sigma(n) \sim$ constant (i.e., $\mu \sim 1/n$) – see Table I for details. Theory predicts (Table I) that for $k_F d \gg 1$, i.e., remote Coulomb disorder, $\mu(n)$ and $\sigma(n)$ should cross-over to $\mu(n) \sim \sqrt{n}$ and $\sigma(n) \sim n^{3/2}$ in graphene. This clear prediction could be verified by putting an impurity layer (e.g. a SiO_2 film) at various values of d from the graphene layer and measuring $\sigma(n)$ to check if the low-density ($2k_F d \ll 1$) $\sigma(n) \sim n$ behavior indeed crosses over to the high density $\sigma(n) \sim n^{3/2}$ behavior as we predict theoretically. In graphene, with a valley degeneracy of 2, $2k_F d \approx 2.5 \tilde{d}\sqrt{\tilde{n}}$, where $\tilde{d} = d/1000$Å, and $\tilde{n} = n/10^{10}\text{cm}^{-2}$. Hence, for $n = 10^{12}$ cm^{-2} and $d = 100$ Å $2k_F d \approx 2.5$. Thus, the condition $2k_F d \gg 1$ would require an impurity layer at $d \approx 1000$ Å (with consequent very weak Coulomb disorder scattering) which may lead to the complication that the subsequent graphene resistivity will be entirely dominated by any underlying short-range disorder (with $\sigma \sim n^0$), masking any $\sigma \sim n^{3/2}$ behavior arising from charged impurity scattering. One possibility would be to put suspended graphene near a thick layer (of thickness L) of disordered substrate with a 3D charged impurity distribution, which would lead to [see Eqs. (38)–(40):

$$\tau^{-1} = \frac{N_i}{\pi\hbar^2 v_0 k_F^2} \left(\frac{2\pi e^2}{\kappa}\right)^2 \int_0^1 dx \frac{x\sqrt{1-x^2}}{(x+q_s)^2} \left[1 - e^{-2L_0 x}\right] \tag{61}$$

with N_i being the 3D impurities density in the impurity layer and $L_0 = 2k_F L$, giving $\sigma(n) \sim n^{3/2}$ for $k_F L \gg 1$ and $\sigma(n) \sim n$ for $k_F L \ll 1$. Such a 3D impurity layer underneath graphene may manifest the superlinear $\sigma(n) \sim n^{3/2}$ conductivity behavior predicted by the theory, but observing the shallow maximum in the exponent β/α for $k_F d \sim 1$ may still be difficult.

VII. OTHER EFFECTS

In this section, just before our conclusion in the next section, we discuss "other effects" completely left out of our theoretical considerations which may compromise and complicate direct quantitative comparisons between our theory and experiment although we believe that our theoretical conclusions should apply generically to transport in high-mobility 2D semiconductor systems at low enough temperatures.

First, phonon effects are neglected in the theory since we explicitly consider the $T = 0$ situation (in practice, $T = 50 - 300$ mK is the typical low-temperature experimental situation mimicking the $T = 0$ theoretical situation). For consistency between theory and experiment, the transport data must therefore be taken at a fixed temperature $T < T_{BG}$, where T_{BG} is the so-called Bloch-Grüneisen temperature, so that acoustic phonon scattering contribution to the resistivity is negligible compared with disorder scattering even in the high-mobility 2D semiconductor structures under consideration in this work. (Optical phonon transport is of no relevance for low-temperature transport since $k_B T \ll \hbar\omega_{LO}$ is explicitly satisfied as $\hbar\omega_{LO} > 100$ K typically.) T_{BG} is given either by the Debye temperature (for 3D metals) or by the energy of the acoustic phonons with $2k_F$-wave vector (for 2D semiconductors), whichever is lower. We therefore have $k_B T_{BG} = 2\hbar k_F v_{ph}$ where v_{ph} is the relevant acoustic phonon velocity in the material. Putting in the appropriate sound velocity (v_{ph}), we get $T_{BG} \approx 2\sqrt{\tilde{n}}$ K; $10\sqrt{\tilde{n}}$ K in 2D GaAs and graphene, respectively, where $\tilde{n}$ is measured in units of 10^{10} cm^{-2}. Thus, down to carrier density $n \sim 10^9$ cm^{-2}, it is reasonable to ignore phonon effects in transport at $T \approx 100$ mK. Acoustic phonon scattering has been considered elsewhere in the literature[8].

Second, we have used the Born approximation in calculating the scattering time and the RPA in calculating the screened Coulomb disorder throughout. Both of these approximations surely become increasingly quantitatively inaccurate at lower carrier density although they should remain qualitatively valid unless there is a metal-insulator transition (obviously, our Drude-Boltzmann transport theory would not apply at or below any metal-insulator transition density). RPA screening theory becomes increasingly quantitatively inaccurate as carrier density (or the corresponding $r_s \sim n^{-1/2}$ parameter) decreases (increases), but there is no well-accepted systematic method for incorporating low-density electronic correlation effects going beyond RPA screening. Including low-density correlation effects in Hubbard-type local field theories do not change any of our qualitative conclusion. As for multiple scattering effects[31] beyond Born approximation, they typically lead to higher-order corrections to the resistivity so that $\rho \propto n_i$, where n_i is the impurity density, is no longer valid and one must incorporate high-order nonlinear corrections to the resistivity going as $O(n_i^2)$ and higher. These nonlinear multiscattering corrections become quantitatively important for $n \lesssim n_i$, and can be neglected for $n > n_i$ regime, which is of our main interest in this paper. Our neglect of multiscattering corrections beyond Born approximation is consistent with our neglect of strong localization effect, both of which will become important in the very low carrier density regime ($n < n_i$) where the Drude-Boltzmann theory becomes manifestly inapplicable.

Third, we ignore all nonlinear screening effects, which have been much discussed in the recent graphene literature[32] where charged impurity induced inhomogeneous electron-hole puddle formation plays an important role at low carrier density, since they are important only at very low carrier density ($n < n_i$) where our whole Boltzmann theoretical approach becomes suspect any way. For the same reason we also do not take into account any scattering-screening self-consistency effect[33] which may also become important at very low carrier

density (again, for $n < n_i$).

Fourth, we ignore any possible spatial correlation effects among impurity locations, assuming the disorder to arise from completely uncorrelated random impurity configurations. If the impurities are spatially correlated, it is straightforward to include the correlation effect in the Boltzmann transport calculation by simply multiplying the disorder potential term in Eq. (8) by the corresponding structure factor $s(q)$ for the impurity distribution, i.e., by writing $|V_q|^2 \to |V_q|^2 s(q)$ in Eq. (8) where

$$s(q) = \frac{1}{n_i} \left| \sum_{i=1}^{n_i} e^{-i\mathbf{q}\cdot\mathbf{r_i}} \right|^2 - n_i \delta_{q0}, \tag{62}$$

where $\mathbf{r_i}$ denotes the position of each impurity and the sum going over all the impurities. This, if experimental information about impurity correlations exists, it is then straightforward to include such spatial correlation effects in the Boltzmann transport calculations, as has indeed been done in both 2D GaAs[34] and graphene[35]. Since intrinsic impurity correlation information is typically unavailable, our model of uncorrelated random disorder seems to be the obvious choice from a theoretical perspective since it involves only one (the impurity density n_i) or two (n_i and the impurity location d) unknown parameters (and most often d is known from the modulation doping setback distance and is thus not a free parameter) whereas including impurity spatial correlations would invariably involve the introduction of more unknown free parameters making the theory of dubious theoretical relevance. Since our interest in this paper is not an absolute calculation of the conductivity or mobility (and hence n_i typically drops out of our theory if only one dominant scattering mechanism is operational), but obtaining the universal density dependence of conductivity, it is important to mention that the main effect of impurity correlation is to suppress the effect of n_i on the resistivity without much affecting the carrier density dependence particularly for $n > n_i$ regime of our interest. We mention that any intrinsic impurity correlations actually increase the value of mobility from our uncorrelated random disorder theory and thus compensate to some extent the suppression of mobility arising from some of the effects discussed above.

Fifth, for our $T = 0$ theory to be strictly applicable to the experimental data, the experimental temperature T should satisfy the condition $T \ll T_F$, where $T_F \equiv E_F/k_B$ is the corresponding Fermi temperature of the system. Using the known dependence of E_F on the 2D carrier density n we see that this implies $T(K) \ll 4.2\tilde{n}$ for 2D n-GaAs, $T(K) \ll 1\tilde{n}$ for 2D p-GaAs, and $T(K) \ll 150\sqrt{\tilde{n}}$ for graphene where $\tilde{n} = n/10^{10}\text{cm}^{-2}$. Thus, low-temperature experiments carried out at $T = 100$ mK satisfy our $T = 0$ theoretical constraint very well down to 10^9 cm^{-2} carrier density (except for 2D p-GaAs hole system where the density cut off is perhaps 5×10^9 cm^{-2}). Our direct numerical calculations at finite temperatures (not shown in this paper) show that our calculated exponents $\alpha(n)$ and $\beta(n) = \alpha + 1$ at $T = 0$ continue to be quantitatively accurate upto $T \gtrsim T_F$ as long as the experimental data for density dependence are taken at a fixed temperature. Thus our theory and numerics for $\alpha(n)$ and $\beta(n)$ are quite robust against thermal effects as long as phonons are unimportant (i.e., $T < T_{BG}$ is satisfied).

We conclude this section of "other effects" by noting that the most important drawback of our RPA-Drude-Boltzmann theory is that it may fail systematically at low carrier density ($n \lesssim n_i$) where important physical effects (which are difficult to treat theoretically) such as strong localization, metal-insulator transition, nonlinear screening, inhomogeneous puddle formation, multiscattering corrections, screening-scattering self-consistent, etc. may all come into play making both our theory inapplicable to the experimental situation. We do, however, anticipate our theory to be applicable to very low carrier densities ($n \gtrsim 10^9$ cm^{-2}) in ultra-high mobility 2D GaAs and graphene systems where $n_i \lesssim 10^8$ cm^{-2} typically. A convenient experimental measure of the applicability of our theory is looking at the dimensionless quantity '$k_F l$' where l is the elastic mean free path defined by $l \equiv v_F\tau$ where τ and v_F are respectively the transport relaxation time and Fermi velocity. We find that $k_F l = 4.14\tilde{n}\tilde{\mu}$ for 2D GaAs systems, where $\tilde{n} = n/10^{10}\text{cm}^{-2}$ and $\tilde{\mu} = \mu/(10^6$ cm^2/Vs) whereas $k_F l = 0.2\tilde{n}\tilde{\mu}$ for graphene. As long as $k_F l > 1$, our Drude-Boltzmann theory should be valid qualitatively and we therefore conclude that the theory remains quantitatively accurate for $n \gtrsim 10^{10}$ cm^{-2} (10^{11} cm^{-2}) for 2D GaAs (graphene) systems in high-quality/high-mobility samples. Thus, there is a large range of carrier density ($10^{10} - 10^{12}$ for 2D GaAs and $10^{11} - 10^{13}$ for graphene) where our predictions for universal density dependence can be experimentally tested through low-temperature transport measurements.

The fact that all the "other effects" left out of our theory affects transport at low carrier densities indicates that our predicted density scaling of conductivity will systematically disagree with the experimental data at lower carrier densities. Of course, "lower" density is a relative term, and the dimensionless quantities such as n/n_i and $k_F l$ are the appropriate quantities to define the regime of validity of our theory. As n/n_i and/or $k_F l$ (or even T_F/T or T_{BG}/T) become smaller, the Drude-Boltzmann theoretic predictions become increasingly unreliable. Nevertheless, the theory remains predictive down to 10^{10} cm^{-2} carrier density (or lower) in high quality (i.e. low values of n_i) GaAs samples at low temperatures ($T \approx 100$ mK).

VIII. DISCUSSION AND CONCLUSION

We have developed a detailed quantitative theory for the density-dependence of the zero-temperature conductivity (or equivalently mobility) of (mainly) 2D and 3D

electron and hole metallic systems assuming transport to be limited by (mainly Coulomb) disorder scattering within the semiclassical Drude-Boltzmann transport theory. We neglect all quantum interference (hence localization) effects as well as interaction effects (except for the carrier screening of the bare impurity Coulomb disorder, which is an essential qualitative and quantitative ingredient of our theory) assuming them to be small since our interest is the density dependence (rather than the temperature dependence) of transport properties at low fixed temperatures in high-mobility ($k_F l \gg 1$ where l is the elastic mean free path) samples.

We have systematically considered 3D and 2D doped (n- and p-) semiconductor systems as well as 2D graphene but the primary focus has been on n-GaAs and p-GaAs quantum well based 2D electron or hole systems, mainly because these systems continue to be of great interest in physics and because the carrier density can easily be tuned in such high-mobility 2D semiconductor systems, and the mobility is dominated by Coulomb disorder at low temperatures. We have taken into account both long-range Coulomb disorder from charged impurities and zero-range disorder arising from possible non-Coulombic short range scatterers. The primary focus has been the Coulombic disorder since this is the main low-temperature resistive scattering mechanism in semiconductors. Instead of discussing the nonuniversal values of μ (and σ), which depend[17] on the actual impurity content, we focus on the universal power-law density scaling of transport properties: $\sigma(n) \sim n^{\beta(n)}$ and $\mu(n) \sim n^{\alpha(n)}$ with $\beta = \alpha + 1$. These exponents α and β are sample-independent and depend only on the nature of the dominant disorder. We provide asymptotic theoretical analysis of α and β (for various types of underlying disorder) in the high and the low density regime and for near and far impurities. We have then verified our analytical results with direct numerical calculations based on the full solution of the Boltzmann transport theory in the presence of disorder scattering.

Although our work is primarily theoretical, we provide a critical comparison with various experimental results in the literature (in 2D n-GaAs electrons and p-GaAs holes), finding generally good agreement between our theoretically predicted exponents α and β and low-temperature experimental findings in high-mobility 2D electron and hole systems. In particular, a truly exciting prediction, that $\alpha(n)$ has a maximum universal value $\alpha_{\max} \sim 1.7$ for all 2D systems at an intermediate carrier density value (approximately defined by $k_F d \sim 1$), seems to be consistent with recent (and old) experimental results from several different groups (and for both 2D electrons and holes), as discussed in details in Sec. VI.

Our theory predicts $\alpha(n)$ to vary from $\alpha = 0$ in the low-density strong-screening regime ($q_{TF} \gg 2k_F$, $n \to 0$) to $\alpha = 3/2$ in the high density weak screening regime ($q_{TF} \ll 2k_F$, $n \to \infty$) with a shallow maximum of $\alpha \sim 1.7$ at intermediate carrier density for $k_F d \sim 1$ where d is the impurity location. Although our work presented in this article is purely theoretical describing the density dependent and disorder-limited $T = 0$ conductivity of 2D/3D carriers using the semiclassical Boltzmann theory approach, it is worthwhile to speculate about the prospects for the experimental observation of our asymptotic low ($\alpha \to$; $\beta \to 1$) and high ($\alpha \to 3/2$; $\beta \to 5/2$) density behavior of Coulomb disorder limited 2D semiconductor transport. These limiting exponents are theoretically universal.

We first summarize the current experimental status in the context of our theory. For scattering by background Coulomb disorder (i.e., near impurities with $2k_F d < 1$), $\alpha(n) \approx 0.5 - 0.8$ typically, and for scattering by remote impurities ($2k_F d > 1$) in the modulation doping layer $\alpha(n) > 1 - 1.3$ typically with a few atypical cases showing $\alpha(n) \sim 1.7$ ($> 3/2$) around $k_F d \sim 1$. All of these are intermediate density results in our theory where q_s ($= q_{TF}/2k_F$) and $2k_F d$ are neither extremely large nor extremely small. Thus the basic experimental situation is in excellent agreement with our theory as it should be because the 2D doped semiconductor transport (as well as graphene) is known to be dominated by screened Coulomb disorder with near or far charged impurities being the dominant scattering mechanism depending on the sample and carrier density.

First, we discuss the high-density situation which is theoretically more straightforward and where the Boltzmann theory is almost exact. As carrier density increases, the semiclassical Boltzmann theory becomes increasingly more valid for Coulomb disorder limited transport properties since the conductivity itself and consequently $k_F l$ increases, thus making the system progressively more metallic. In addition, increasing density decreases the metallic r_s-parameters, the dimensionless Wigner-Seitz radius, given by $r_s = me^2/(\kappa\hbar^2\sqrt{\pi n})$ for 2D semiconductor systems. Since $r_s \sim n^{-1/2}$, at high carrier density (e.g., $r_s = 0.5$, 2.5 for 2D n-GaAs, p-GaAs respectively at $n = 10^{12}$ cm^{-2}) r_s is small, making our theory using RPA screened effective Coulomb disorder to be systematically more valid at higher carrier density as RPA becomes exact at low r_s. Thus, it appears that the ideal applicability of our theory is in obtaining the high-density 2D system.

This is indeed true except that new physical (rather than theoretical) complications arise making it problematic for a direct comparison between our theory and experiment on 2D systems at high carrier density. Two new elements of physics come into play at high carrier density, both contributing to the suppression (enhancement) of mobility (scattering rate): Intersubband scattering becomes important as the Fermi level moves up and comes close to (or crosses over into) the higher confined subbands of the quasi-2D quantum well, thus opening up a new scattering channel; and, short-range scattering at the interface and by alloy disorder (in AlGaAs) becomes important as the self-consistent electric field created by the electrons themselves pushes the carriers close to the interface at high carrier density. Both of these physical effects eventually suppress the monotonic growth of

$\mu(n)$ and $\sigma(n)$ with increasing density, and eventually $\mu(n)$ starts decreasing with increasing carrier density at high enough density (for $n > 3 \times 10^{11}$ cm^{-2} in GaAs-AlGaAs systems) instead of continuing as $\mu(n) \sim n^{3/2}$ as it would in the high-density regime if Coulomb disorder is the only dominant scattering mechanism with no other complications. Since at high density $\tau^{-1}(n) \sim n^{\alpha}$ with $\alpha > 1$ for Coulomb disorder, eventually at some (nonuniversal sample dependent) high density, Coulomb disorder becomes insignificant compared with the short-range scattering effects. Obviously, the density at which this happens is non-universal and depends on all the details of each sample. But in all 2D systems and samples, eventually, when Coulomb disorder induced scattering rate is sufficiently small, a high density regime is reached where the mobility stops increasing (and even starts decreasing). In Si MOSFETs[10] this effect is very strong already around $\sim 10^{12}$ cm^{-2} because of considerable surface roughness scattering at the Si-SiO_2 interface, and $\mu(n)$ decreases with increasing n at higher density. Even in high-mobility GaAs systems, $\mu(n)$ saturates (i.e., $\alpha = 0$) and eventually starts decreasing at a nonuniversal density around $n \gtrsim 3 \times 10^{11}$ cm^{-2}. Boltzmann transport theory can be easily generalized to incorporate inter-subband scattering and surface scattering, but the physics is nonuniversal and beyond the scope of our current work.

The low-density ($n \to 0$) situation is fundamentally inaccessible to our Boltzmann transport theory since all doped semiconductor systems (3D or 2D) eventually undergo an effective metal-insulator transition at (a nonuniversal) low (critical) density with the semiclassical Boltzmann theory eventually becoming invalid as a matter of principle at a sufficient low sample-dependent carrier density. In 3D, this transition may be a true Anderson localization transition as $k_F l \to 1$ with decreasing density making the Boltzmann theory inapplicable. In 2D semiconductors, which are the systems of our main interest, the observed metal-insulator transition at a nonuniversal sample dependent critical density n_c is likely to be a crossover phenomenon[5,9] since the scaling theory of Anderson localization predicts 2D to be the critical dimension with no localization transition. There is considerable experimental support for the observed low-density 2D metal-insulator transition to be a density inhomogeneity-driven percolation transition at a nonuniversal critical density n_c where charged impurity induced Coulomb disorder drives the system into an inhomogeneous collection of "puddles" with a mountain and lake potential landscape where semiclassical metallic transport becomes impossible for $n < n_c$ with n_c being the disorder-dependent percolation transition density[20,21,36–38]. The critical density n_c depends crucially on the sample quality and is typically below 10^9 cm^{-2} in high-mobility GaAs systems — in Si MOSFETs, where disorder is very strong, $n_c \approx 10^{11}$ cm^{-2}, and this is why we have left out 2D Si systems from our consideration in this work although our basic theory applies well to 2D Si-based systems for $n > 10^{11}$ cm^{-2}.

Our semiclassical Boltzmann theory works for $n \gg n_c$, but for $n \to n_c$, one must include the inhomogeneous puddle formation and the associated percolation transition even in the semiclassical theory[39]. This is the reason our theory fails for real 2D systems in the $n \to 0$ limit unless the level of disorder is extremely low (even then our Boltzmann theory is valid only for $n \gg n_c$ and the $n \to 0$ limit is fundamentally inaccessible).

In spite of this fundamental difficulty in accessing the low-density (i.e. $n \to 0$) limit using our theory directly, it turns out that we can approximately include the effect of a semiclassical percolation transition in our theory by an indirect technique in the density regime $n > n_c$ above the effective metal-insulator transition (but still in a reasonably low density regime for high-quality samples where n_c can be very low). Since the percolation picture essentially eliminates a certain fraction of the carriers from being metallic, we can assume that the effective conductivity (mobility) for $n \gg n_c$ is given by the same exponent β (α) calculated in our theory with the only caveat that β (α) is now the exponent only for the actual "metallic" free mobile carrier fraction of the whole system. We can then write:

$$\mu = A(n - n_c)^{\alpha} = Bn^{\alpha'}, \tag{63}$$

where $\alpha(n)$ is the real exponent we calculate theoretically from the Boltzmann theory and $\alpha'(n)$ is the effective (apparent) exponent obtained experimentally from

$$\alpha'(n) = \frac{d \ln \mu(n)}{d \ln n} \tag{64}$$

by using the actual data for $\mu(n)$ without taking into account any complications arising from the existence of n_c. Using Eqs. (63) and (64), we immediately get the following relationship connecting the effective exponent α' with the real exponent α for $n \gg n_c$

$$\alpha' = \alpha(1 - n_c/n)^{-1}, \tag{65}$$

for $n \gg n_c$. We note that $\alpha' \approx 2\alpha$ for $n = 2n_c$. Eq. (65) is valid within logarithmic accuracy, and connects the measured low-density (n small, but $n \gg n_c$ being still valid) exponent $\alpha'(n)$ with the real Boltzmann theory exponent (as in Table I) $\alpha(n)$. Since n_c can be measured experimentally by checking where $\sigma(n)$ vanishes, and defining n_c to be $\sigma(n_c) = 0$ at $T = 0$, we then immediately see that the measured low-density effective exponent $\alpha'(n) > \alpha(n)$ always, and in fact, $\alpha'(n) \to \infty$ as $n \to n_c^+$. Thus, we conclude that the experimentally measured mobility exponent will eventually start increasing as n decreases approaching n_c. For $n \gg n_c$, we get $\alpha' \approx \alpha$, but the leading correction to α goes as $\alpha' = \alpha(1 + n_c/n)$ for $n \gg n_c$. We note that the existence of n_c enhances α over its nominal value of Table I even for $n \gg n_c$!

We have checked existing experimental results in the literature (to the extent n_c, α' etc. are known experimentally), finding that our prediction of Eq. (65) seems

to apply quite well. We note that since the pristine calculated $\alpha(n)$ decreases with decreasing n (see Figs. 1–8) for *all* models of Coulomb disorder at low carrier density, Eq. (65) predicts that the apparent exponent α' would be close to α for $n \gg n_c$, but would then manifest a minimum at a density n_0 ($> n_c$) defined by the equation:

$$\frac{d\alpha}{dn} = \frac{\alpha(n_c/n)}{(n-n_c)} \tag{66}$$

at $n = n_0 > n_c$. For $n < n_0$, α' will increase as n decreases (with α' being a minimum at $n = n_0$), eventually diverging as $(1 - n_c/n)^{-1}$ as $n \to n_c^+$. We find this behavior to be qualitatively consistent with all the existing data in the literature although a precise quantitative comparison necessitates more low temperature data showing $\mu(n)$ all the way down to $n = n_c$ where $\mu(n) = 0$. Careful measurements of $\sigma(n)$ close to n_c are lacking in the literature for us to form a definitive conclusion on this matter at this stage.

We conclude by pointing out that very close to the percolation transition, where $n - n_c \ll n_c$, i.e. $n \ll 2n_c$, we expect the critical behavior of 2D percolation transition to possibly come into play, where the conductivity may have a completely different universal 2D percolation exponent δ (totally distinct from α or α') which has nothing to do with our Boltzmann theory:

$$\sigma \sim (n - n_c)^{\delta} \tag{67}$$

for $(n - n_c) \ll n_c$. This percolation critical exponent δ for $\sigma(n)$ can only manifest itself very close to n_c (i.e. $n \ll 2n_c$), and for $n \gtrsim 2n_c$ we believe that our effective theory predicts an effective conductivity exponent $\beta' = \alpha' + 1$ given by

$$\beta' \approx \frac{\alpha}{1 - n_c/n} + 1 = \frac{\beta - n_c/n}{1 - n_c/n}, \tag{68}$$

for $n \gtrsim 2n_c$. Again, as for α', $\beta' \approx \beta = \alpha + 1$ for $n \gg n_c$. The conductivity exponents δ and β' arise from completely different physics (from percolation critical theory near n_c and Boltzmann theory far above n_c, respectively) and have nothing to do with each other. How the transition or crossover occurs even within the semiclassical theory from β' (for $n \gtrsim 2n_c$) to δ for ($n \ll 2n_c$) is a very interesting question which is beyond the scope of the current work. In our current work, we have, however, solved [Eqs. (63) – (68) above] the problem of the crossover from the effective exponent α' (or β') for $n \gtrsim 2n_c$ to the true Boltzmann exponent α (or β) for $n \gg 2n_c$.

We give one possible experimental example for the observed crossover from the Boltzmann exponent α (for $n \gg n_c$) to α' (for $n \gtrsim n_c$) arising in Jiang *et al.*[40]. In this work[40], the conductivity was measured in a high-mobility modulation doped 2D GaAs electron system, finding the effective mobility exponent $\alpha \approx 0.9 - 1.1$ in the high density range ($n \sim 5\times10^{10} - 3\times10^{11}$ cm^{-2}) for $d = 350 - 750$ Å. This range of n and d converts to $2k_F d = 1 - 5$ and $q_s \approx 1$, which is the intermediate density range for all our Coulomb disorder mechanisms in Table I. Given that the measured mobility in Ref. [40] was relatively modest, $\mu \sim 10^5 - 10^6$ cm^2/Vs, it is reasonable to expect, based on our numerical mobility calculations, for both remote and background Coulomb scattering to be equivalently effective, leading to $\alpha \sim 0.9 - 1.2$ according to our numerical results of Sec. IV. Thus, the "high-density" exponent ($\alpha \sim 1$) in the Jiang sample agrees well with our theory. The interesting point to note in the current context is that Jiang *et al.*[40] found a large increase of the measured exponent α as n decreases, which is in apparent disagreement with our analytical theory which always gives $\alpha(n)$ decreasing with decreasing n. Although other possibilities (e.g., multiscattering) cannot be ruled out[31], we believe that the Jiang *et al.* data indicate a crossover from α to α' as n decreases. In particular, the measured mobility exponent increased from $\alpha \sim 1$ to $\alpha \sim 4$ as n decreased from $\sim 10^{11}$ cm^{-2} to $\sim 2 \times 10^{11}$ cm^{-2} (with also a factor of 50 decrease in mobility). Assuming $n_c \sim 1.5 \times 10^{11}$ cm^{-2} (which is consistent with the data), we get [from Eq. (65)], $\alpha' \approx 4\alpha \approx 4$ at $n \approx 2\times10^{10}$ cm^{-2}, which is in excellent agreement with the data[40]. We therefore believe that the Jiang *et al.* experiment manifests our predicted crossover behavior from $\alpha(n)$ to $\alpha'(n)$ as n approaches n_c from above.

We note that $k_F l \approx 1$ in the Jiang *et al.* sample for $n \approx 3 \times 10^{10}$ cm^{-2} (where $\mu \approx 10^5$ cm^2/Vs seems to have been reached starting from $\mu \sim 10^6$ cm^2/Vs for $n \sim 3 \times 10^{11}$ cm^{-2}), and thus the identification of $n_c \approx 1.5\times10^{10}$ cm^{-2} is meaningful. Clearly, our simple Drude-Boltzmann theory applies for $n \gg 3 \times 10^{10}$ cm^{-2}, but not for $n < 3 \times 10^{10}$ cm^{-2} where $k_F l \sim 1$. What is encouraging is that the simple modification of the theory introducing the crossover exponent $\alpha' = \alpha(1 - n/n_c)^{-1}$ seems to describe the experimentally observed density scaling exponent of the observed experimental mobility at low carrier densities.

We conclude by mentioning that direct numerical percolation calculations indicate $\delta \approx 1.32$ in 2D systems, which is unfortunately too close to our calculated value of β in the low-density Coulomb disorder-dominated Boltzmann theory, where (see Figs. 1 – 6 and 8) the low-density ($n \lesssim 10^{10}$ cm^{-2}) α-value is $\alpha \approx 0.3 - 0.5$ implying low-density $\beta \approx 1.3 - 1.5$. Since high-mobility 2D GaAs samples typically have $n_c \approx 10^9$ cm^{-2}, it is unclear whether the existing conductivity exponent measurements for the putative metal-insulator transition[20,21,36,37] for the 2D density-driven metal-insulator transition really is obtaining δ or is just a measurement of our calculated $\beta = \alpha + 1$ which at low values of n would be rather close to the experimentally measured percolation exponent of $1.3 - 1.5$. The current experiments do not really quantitatively measure $\sigma(n)$ in the $n < 2n_c$ regime necessary for obtaining δ, and we feel that much more work will be needed to establish the nature of the $\sigma(n \to n_c) \to 0$ transition observed in the laboratory. It is possible, even likely, that the existing measurements have only measured the low

density (but still $n \gg n_c$) value of our calculated (non-critical) Boltzmann exponent $\beta \approx 1.3 - 1.5$ in n- and p-2D GaAs systems.

In conclusion, we have developed a comprehensive theory for the universal density scaling of the low-temperature transport properties of 2D and 3D doped semiconductors and graphene, concentrating on the role of background Coulomb disorder and obtaining, both theoretically and numerically, the power law exponents for the density-dependent mobility and conductivity within the Boltzmann transport theory.

ACKNOWLEDGMENTS

This work was supported by Microsoft Q, JQI-NSF-PFC, DARPA QuEST, LPS-CMTC, and US-ONR.

[1] We cite here some representative papers for the theoretical calculation of the impurity resistivity in 3D metals in the context of metallic residual resistivity. See, for example, V. U. Nazarov, G. Vignale, and Y.-C. Chang, arXiv:1302.1660 (2013) and references therein; M. J. Puska and R. M. Nieminen, Phys. Rev. B **27**, 6121 (1983); Yu. Yu. Tsiovkin, A. N. Voloshinskii, V. V. Gapontsev, and V. V. Ustinov, Phys. Rev. B **71**, 184206 (2005); J. P. Dekker, A. Lodder, and J. van Ek, Phys. Rev. B **57**, 12719 (1998); Raju P. Gupta, Phys. Rev. B **35**, 5431 (1987); John H. Tripp and David E. Farrell, Phys. Rev. B **7**, 571 (1973); P. T. Coleridge, N. A. W. Holzwarth, and Martin J. G. Lee, Phys. Rev. B **10**, 1213 (1974); A. R. DuCharme and L. R. Edwards, Phys. Rev. B **2**, 2940 (1970).

[2] Neil W. Ashcroft and N. David Mermin, *Solid State Physics* (Sannders, Orlando, 1976); N. Mott and H. Jones, *The Theory of the Properties of Metals and Alloys* (Clarendon, Oxford, 1936).

[3] Y. Hanein, U. Meirav, D. Shahar, C. C. Li, D. C. Tsui, and Hadas Shtrikman, Phys. Rev. Lett. **80**, 1288 (1998); M. Y. Simmons, A. R. Hamilton, M. Pepper, E. H. Linfield, P. D. Rose, D. A. Ritchie, A. K. Savchenko, and T. G. Griffiths, Phys. Rev. Lett. **80**, 1292 (1998); A. P. Mills, Jr., A. P. Ramirez, L. N. Pfeiffer, and K. W. West, Phys. Rev. Lett. **83**, 2805 (1999); X. P. A. Gao, G. S. Boebinger, A. P. Mills, Jr., A. P. Ramirez, L. N. Pfeiffer, and K. W. West, Phys. Rev. Lett. **94**, 086402 (2005).

[4] Y. Hanein, D. Shahar, J. Yoon, C. C. Li, D. C. Tsui, and Hadas Shtrikman, Phys. Rev. B **58**, R13338 (1998); M. P. Lilly, J. L. Reno, J. A. Simmons, I. B. Spielman, J. P. Eisenstein, L. N. Pfeiffer, K. W. West, E. H. Hwang, and S. Das Sarma, Phys. Rev. Lett. **90**, 056806 (2003); J. Zhu, H. L. Stormer, L. N. Pfeiffer, K. W. Baldwin, and K. W. West, Phys. Rev. Lett. **90**, 056805 (2003); Xiaoqing Zhou, B. Schmidt, L. W. Engel, G. Gervais, L. N. Pfeiffer, K. W. West, and S. Das Sarma, Phys. Rev. B **85**, 041310(R) (2012).

[5] S. Das Sarma and E. H. Hwang, Phys. Rev. Lett. **83**, 164 (1999); Phys. Rev. B **69**, 195305 (2004); Phys. Rev. B **61**, R7838 (2000); Solid State Commun. **135**, 579 (2005).

[6] G. Zala, B. N. Narozhny, and I. L. Aleiner, Phys. Rev. B **64**, 214204 (2001); B. Altshuler and D. Maslov, Phys. Rev. Lett. **82**, 145 (1999).

[7] S. Das Sarma, Phys. Rev. B **33**, 5401 (1986); A. Gold and V. Dolgopolov, Phys. Rev. B **33**, 1076 (1986); F. Stern, Phys. Rev. Lett. **44**, 1469 (1980).

[8] T. Kawamura and S. Das Sarma, Phys. Rev. B —bf 42, 3725 (1990); Phys. Rev. B **45**, 3612 (1992); E. H. Hwang and S. Das Sarma, Phys. Rev. B **77**, 115449 (2008); Hongki Min, E. H. Hwang, and S. Das Sarma, Phys. Rev. B **86**, 085307 (2012).

[9] See, for example, S. Das Sarma, S. Adam, E. H. Hwang, and E. Rossi, Rev. Mod. Phys. **83**, 407 (2011), and references therein.

[10] T. Ando, A. B. Fowler, and F. Stern, Rev. Mod. Phys. **54**, 437 (1982).

[11] E. Conwell and V. F. Weisskopf, Phys. Rev. **77**, 388 (1950); R. Dingle, Phil. Mag. **46**, 831 (1955).

[12] D. Chattopadhyay and H. J. Queisser, Rev. Mod. Phys. **53**, 745 (1981); K. Seeger, *Semiconductor Physics* (Springer, Berlin, 1986); B. Nag, *Electron in Compound Semiconductor* (Springer, Berlin, 1986); F. Blatt, *Physics of Electronic Conduction in Solids* (McGraw-Hill, New York, 1968); B. Ridley, *Quantum Processes in Semiconductors* (Oxford, Oxford, 1982).

[13] Frank Stern, Phys. Rev. Lett. **18**, 546 (1967).

[14] J. Lindhard, Kgl. Danske Videnskab. Selskab, Mat.-Fys. Medd. **28**, No. 8 (1954).

[15] E. H. Hwang and S. Das Sarma, Phys. Rev. B **75**, 205418 (2007)

[16] E. H. Hwang, S. Adam, and S. Das Sarma, Phys. Rev. Lett. **98**, 186806 (2007).

[17] E. H. Hwang and S. Das Sarma, Phys. Rev. B **77**, 235437 (2008).

[18] H. L. Stormer, Z. Schlesinger, A. Chang, D. C. Tsui, A. C. Gossard, and W. Wiegmann, Phys. Rev. Lett. **51**, 126 (1983); R. C. Miller, D. A. Kleinman, and A. C. Gossard, Phys. Rev. B **29**, 7085 (1984); D. A. Broido and L. J. Sham, Phys. Rev. B **31**, 888 (1985); Y.-Ch. Chang and R. B. James, Phys. Rev. B **39**, 12672 (1989); R. Ferreira and G. Bastard, Phys. Rev. B **43**, 9687 (1991).

[19] Y.-W. Tan, Y. Zhang, K. Bolotin, Y. Zhao, S. Adam, E. H. Hwang, S. Das Sarma, H. L. Stormer, and P. Kim, Phys. Rev. Lett. **99**, 246803 (2007); J.-H. Chen, C. Jang, S. Adam, M. S. Fuhrer, E. D. Williams, and M. Ishigami Nature Physics **4**, 377 (2008).

[20] S. Das Sarma, M. P. Lilly, E. H. Hwang, L. N. Pfeiffer, K. W. West, and J. L. Reno, Phys. Rev. Lett. **94**, 136401 (2005).

[21] M. J. Manfra, E. H. Hwang, S. Das Sarma, L. N. Pfeiffer, K. W. West, and A. M. Sergent, Phys. Rev. Lett. **99**, 236402 (2007).

[22] R. H. Harrell, K. S. Pyshkin, M. Y. Simmons, D. A. Ritchie, C. J. B. Ford, G. A. C. Jones, and M. Pepper, Appl. Phys. Lett. **74**, 2328 (1999).

[23] M. R. Melloch, Thin Solid Films, **231**, 74 (1993).

[24] Loren Pfeiffer, K. W. West, H. L. Stormer, and K. W. Baldwin, Appl. Phys. Lett. **55**, 1888 (1989).

[25] M. Shayegan, V. J. Goldman, C. Jiang, T. Sajoto, and M. Santos, Appl. Phys. Lett. **52**, 1086 (1988).

[26] Kazuhiko Hirakawa and Hiroyuki Sakaki, Phys. Rev. B **33**, 8291 (1986).
[27] L. Pfeiffer and K. West, private communication and unpublished.
[28] J. D. Watson, S. Mondal, G. A. Csthy, M. J. Manfra, E. H. Hwang, S. Das Sarma, L. N. Pfeiffer, and K. W. West, Phys. Rev. B **83**, 241305 (2011).
[29] J. D. Watson, S. Mondal, G. Gardner, G. A. Csathy, and M. J. Manfra, Phys. Rev. B **85**, 165301 (2012).
[30] S. Das Sarma and E. H. Hwang, Phys. Rev. B **87**, 035415 (2013); S. Das Sarma, E. H. Hwang, and Qiuzi Li, Phys. Rev. B **85**, 195451 (2012).
[31] A. Gold, Appl. Phys. Lett. **54**, 2100 (1989).
[32] S. Adam, E.H. Hwang, V.M. Galitski, and S. Das Sarma, Proc. Natl. Acad. Sci. U.S.A. **104**, 18392 (2007); E. Rossi and S. Das Sarma Phys. Rev. Lett. **107**, 155502 (2011).
[33] S. Das Sarma, Phys. Rev. Lett. **50**, 211 (1983).
[34] T. Kawamura and S. Das Sarma, Solid State Commun. **100**, 411 (1996); E. Buks, M. Heiblum, and Hadas Shtrikman, Phys. Rev. B **49**, 14790 (1994); S. Das Sarma and S. Kodiyalam, Sem. Sci. Tech. **13**, A59-A62 (1988).
[35] Qiuzi Li, E. H. Hwang, E. Rossi, and S. Das Sarma, Phys. Rev. Lett. **107**, 156601 (2011); Jun Yan and Michael S. Fuhrer, Phys. Rev. Lett. **107**, 206601 (2011).
[36] R. Leturcq, D. LHote, R. Tourbot, C. J. Mellor, and M. Henini, Phys. Rev. Lett. **90**, 076402 (2003); Y. Meir, *ibid.* **83**, 3506 (1999)
[37] L. A. Tracy, E. H. Hwang, K. Eng, G. A. Ten Eyck, E. P. Nordberg, K. Childs, M. S. Carroll, M. P. Lilly, and S. Das Sarma, Phys. Rev. B **79**, 235307 (2009).
[38] S. Adam, S. Cho, M. S. Fuhrer, and S. Das Sarma, Phys. Rev. Lett. **101**, 046404 (2008).
[39] E. H. Hwang and S. Das Sarma, Phys. Rev. B **82**, 081409 (2010); Q. Li, E. H. Hwang, and S. Das Sarma, Phys. Rev. B **84**, 115442 (2011).
[40] C. Jiang, D. C. Tsui, and G. Weimann, Appl. Phys. Lett. **53**, 1533 (1988).